Chemical and Electrochemical Investigations of Cobalt Cyanide and Ruthenium Ammine Complexes

Thesis by

Hong Sup Lim

In Partial Fulfillment of the Requirements
For the Degree of
Doctor of Philosophy

California Institute of Technology
Pasadena, California

1972
(Submitted July 27, 1971)

To my parents and wife

ACKNOWLEDGMENTS

I wish to express my sincere gratitude to my research advisor, Fred C. Anson, for his continuous encouragement and advice, both in research and personal matters. It is a pleasure to acknowledge, with thanks, Professors Harry B. Gray and Jack Halpern for their critical and helpful discussions on my research.

I wish to thank Professor Joseph G. Gordon II for his help in the preparation of this thesis. I would also like to thank Dr. Donald J. Barclay for his help and advice during the early phase of my work.

I wish to acknowledge the aid and friendship I have received from the members of Professor Anson's and Professor Gray's research groups during the course of my study at Caltech. They are (in alphabetical order) Drs. Roger H. Abel, Josip Caja, Predoctor Steven N. Frank, Drs. Jeffrey L. Huntington, Dusan Konrad, Robert A. Levenson, Eduardo A. Neves, Robert S. Rogers, George S. Rossman, Youn Soo Sohn, V. S. Srinivasan, Chaim Yarnitzky and many others.

I wish to thank Mrs. Harue Bierce for her typing of this thesis.

I wish to thank the California Institute of Technology for its financial support during the period of my studies.

Finally, I want to thank my wife, Kwang Ja, for her patience and understanding during the course of my thesis work.

ABSTRACTS

Part I.

The stoichiometry and kinetics of the reaction between $Co(CN)_5H^{3-}$ and HgX_2 (X = CN , OH) have been investigated. The products of the reaction are two new complexes, $[(NC)_5Co-HgX]^{3-}$ and $[(NC)_5Co-Hg-Co(CN)_5]^{6-}$, whose spectra are reported. The kinetic measurements produced a value for the forward rate constant of the reaction $Co(CN)_5H^{3-} + OH^- \underset{k_{-1}}{\overset{k_1}{\rightleftharpoons}} Co(CN)_5^{4-} + H_2O$, $k_1 = (9.7 \pm 0.8) \times 10^{-2}$ $\underline{M}^{-1}$ sec^{-1} at 24°C, and an equilibrium constant for the reaction $K = 10^{-6}$ $\underline{M}^{-1}$.

Part II.

Unusually large and sharp "adsorption waves" appear in cyclic voltammograms of $Co(CN)_5^{3-}$ and several cobalt(III) pentacyano complexes at stationary mercury electrodes. The nature of the adsorbed species and the reasons for the absence of the adsorption waves in polarograms taken with a d. m. e. have been examined. The data are compatible with the adsorption, in all cases, of a coordinatively unsaturated cobalt(II) complex, $Co(CN)_4^{2-}$, by means of a cobalt-mercury bond. When the resulting adsorbed complex is reduced, a series of subsequent chemical and electrode reactions is initiated in which three faradays of charge are consumed for each mole of adsorbed complex. The adsorption of the anionic complex

strongly retards the reduction of other negatively charged complexes.

Part III.

A number of formal redox potentials for $Ru^{III}(NH_3)_5L + e = Ru^{II}(NH_3)_5L$ and $Ru^{III}(NH_3)_4L_2 + e = Ru^{II}(NH_3)_4L_2$ (where L is various ligands) has been measured by cyclic voltammetry, potentiometry, and polarography and are discussed in terms of the properties of the ligands, such as π-accepting capability. Reduction of coordinated pyrazine in the complexes, $Ru(NH_3)_5Pz^{2+}$, cis- and trans-$Ru(NH_3)_4Pz_2^{2+}$, on a mercury electrode has been observed. The behavior of this reduction in various acidity of the solution as well as the reoxidation of the reduction products are discussed.

TABLE OF CONTENTS

Part I. Reactions of Hydridopentacyanocobaltate(III) and Pentacyanocobaltate(II) with Mercury(II) to Form Complexes of the Type $(NC)_5CoHgX^{3-}$ and $(NC)_5CoHgCl(CN)_5^{6-}$

Part I is published in Inorg. Chem., 10, 103 (1971).

REACTIONS OF HYDRIDOPENTACYANOCOBALTATE(III) AND PENTACYANOCOBALTATE(II) WITH MERCURY(II) TO FORM COMPLEXES OF THE TYPE $[(NC)_5Co-HgX]^{3-}$ AND $[(NC)_5Co-Hg-Co(CN)_5]^{6-}$

The electrochemistry of pentacyanocobaltate(II) at mercury electrodes is complicated by an extensive and usually strong adsorption of the reactant on the electrode surface.[1] The remarkable strength of the interaction between the cobalt(II)-cyanide complex and the mercury surface lead us to examine the homogeneous reactions that occur when $Co(CN)_5^{3-}$ or $Co(CN)_5H^{3-}$ are exposed to complexes of Hg(II). Two relatively stable new complexes containing cobalt-mercury bonds were produced by these reactions. The novelty of these complexes and the possibility that they might be involved in the strong adsorption of cobalt-cyanide complexes on mercury electrodes prompted us to investigate the stoichiometry and kinetics of the reactions by which they are formed. The results of these studies are the basis of this report.

EXPERIMENTAL

Reagents

Reagent grade chemicals were used without further purification. Solutions of $Co(CN)_5^{3-}$ were prepared just before they were used by

mixing deaerated solutions of $Co(NO_3)_2$ with stoichiometric quantities of NaCN dissolved in deaerated water. Deaeration was accomplished with pre-purified nitrogen which was further purified by passing it through a washing tower containing V(II) followed by another containing Cr(II).

Solutions of $Co(CN)_5H^{3-}$ were prepared either by treating $Co(CN)_5^{3-}$ with excess hydrogen gas [2] or by reducing solutions of $Co(CN)_5Cl^{3-}$ (prepared according to ref. 3) electrochemically at a mercury pool electrode. For all the quantitative kinetic measurements the electrochemical preparation was employed. The solutions resulting from the electrochemical preparation were analyzed for $Co(CN)_5H^{3-}$ spectrophotometrically at 305 nm. [2]

A stock solution of 8 F $NaClO_4$ was prepared by neutralizing 60% $HClO_4$ with solid Na_2CO_3. After heating overnight on a steam bath and filtering off the siliceous residue, the solution was freed of CO_2 by making it slightly acidic and passing nitrogen gas through it.

Moderately pure solid samples of $K_6[HgCo_2(CN)_{10}]\cdot xH_2O$ were isolated by the following procedure. A 60-ml sample of a 1 F KOH solution containing 7.3 grams (0.11 mole) of KCN was deaerated with hydrogen gas. A 20-ml amount of a deaerated 1 F $CoCl_2$ solution was added and the mixture was stirred by passing hydrogen gas through it. The initially dark-green solution became pale green after ca. 1 hour at which point 2.5 gr (0.01 mole) of solid $Hg(CN)_2$ was added. As the $Hg(CN)_2$ dissolved the solution turned yellowish orange. A 70-ml sample of deaerated absolute ethanol was added to the solution which

caused a reddish orange oil to separate. The oil was transferred with a hypodermic syringe to ca. 10 ml of deaerated absolute ethanol whereupon a yellow solid formed. The solid was crushed, washed several times with ethanol and then with dry ether. It was dried in a vacuum desiccator. Attempts to recrystallize the salt from aqueous solutions were thwarted by apparent decomposition of the complex.

The solid changes color slowly upon exposure to air. Dissolution of the solid in air-free water yielded a spectrum identical with that obtained by treating $Hg(CN)_2$ with an excess of $Co(CN)_5H^{3-}$. Elementary analyses of solid samples resulting from the procedure described gave typical Co:Hg:C:N molar ratios of 2.00:0.95:10.4:10.6.

The reducing equivalents in the solid sample were assayed by means of Andrews titrations[4] of weighed portions. The results corresponded to four reducing equivalents per mole of sample having a molecular weight given by the formula $K_6[HgCo_2(CN)_{10}] \cdot 4H_2O$. Inasmuch as the conditions of the Andrews titration assure that the final oxidation states of the mercury and cobalt are Hg(II) and Co(III), the results obtained correspond to initial oxidation states of either Hg(II) and Co(I) or Hg(0) and Co(II).

A solid sample of what appeared to be $K_6[CdCo_2(CN)_{10}] \cdot xH_2O$ was obtained by a similar procedure in which $Cd(NO_3)_2$ was substituted for $Hg(CN)_2$.

Apparatus

Electronic spectra were recorded with a Cary 14 spectrophotometer or taken manually with a Beckman Model DU spectrophotometer with a Gilford Model 220 Absorbance Indicator attachment. All kinetic runs were performed manually with the latter instrument. A Cary Model 14 CMRI recording spectrophotometer was employed to obtain spectra at low temperatures and infrared spectra were obtained with a Perkin-Elmer Model 225 spectrophotometer. Magnetic susceptibilities were measured with a Princeton Applied Research Model FM-1 vibrating sample magnetometer.

An Orion Model 94-06 cyanide sensitive electrode was used to monitor cyanide activities in some solutions.

Procedure for Kinetic Measurements

The rates of the reaction between $Co(CN)_5H^{3-}$ and $Hg(CN)_2$ were followed spectrophotometrically. Alkaline solutions containing measured quantities of $Hg(CN)_2$ were adjusted to an ionic strength of 0.5 with $NaClO_4$ and deaerated with nitrogen. An aliquot of an air-free solution of $Co(CN)_5H^{3-}$ was added under nitrogen by means of a syringe and the mixture stirred briefly with nitrogen. An aliquot of this mixture was transferred without exposure to air to a spectrophotometer cell which was then placed in the thermostated cell compartment. The absorbances of the reaction products at 274 nm and 362 nm were then recorded manually using a 0.5 F $NaClO_4$ solution as a blank. The small absorbance of $Co(CN)_5H^{3-}$ at 274 nm

was corrected for.

The absorbance-time data were analyzed by conventional least-squares fitting to appropriate kinetic equations. The equations used and the assumptions involved are given in the Results and Discussion Section.

RESULTS AND DISCUSSION

When small increments of $Hg(CN)_2$ are added to alkaline solutions containing an excess of $Co(CN)_5H^{3-}$, an intense absorption band develops with a maximum at ca. 274 nm. This band reaches a maximum intensity some time (depending on the concentrations employed) after the reagents are mixed and then begins to decrease in intensity. At the same time, a new band begins to develop at 362 nm. After the spectrum has become stable the band at 274 nm is absent and the band at 362 nm is found to obey Beer's Law with respect to the amount of $Hg(CN)_2$ added (excess $Co(CN)_5H^{3-}$ being present). At 25°C and $\mu = 1.0$ ($NaClO_4$), the molar absorbance of the band at 362 nm is 52,000 cm^{-1} $\underline{M}^{-1}$.

If the experiment is carried out with more nearly equal concentrations of $Co(CN)_5H^{3-}$ and $Hg(CN)_2$, the band at 362 nm reaches a maximum absorbance with a ratio of $Hg(CN)_2$ to $Co(CN)_5H^{3-}$ of 0.5. When this ratio becomes larger than 0.5, the band that develops initially at 274 nm does not disappear completely when the spectrum has become stable and a corresponding decrease in the absorbance

at 362 nm is observed. At ratios greater than ca. 1.2 no band develops at 362 nm and the band at 274 nm reaches a maximum absorbance which is stable on further standing. The molar absorbance at 274 nm under these conditions amounts to ca. 20,000 cm^{-1} $\underline{M}^{-1}$ based on the concentration of $Co(CN)_5H^{3-}$. Figure 1 shows how the bands at 274 nm and 362 nm change during the period before the spectrum stabilizes. An isosbestic point is observed at ca. 300 nm. Figure 2 summarizes the behavior observed at both wavelengths and is consistent with the following set of overall reactions:

$$Co(CN)_5H^{3-} + Hg(CN)_2 + OH^- \longrightarrow [(NC)_5Co-HgCN]^{3-} + CN^- + H_2O \qquad (1)$$

$$Co(CN)_5H^{3-} + [(NC)_5Co-HgCN]^{3-} + OH^- \longrightarrow [(NC)_5Co-Hg-Co(CN)_5]^{6-} + CN^- + H_2O \qquad (2)$$

with the bands at 274 nm and 362 nm corresponding, respectively, to the ions $[(NC)_5Co-HgCN]^{3-}$ and $[(NC)_5Co-Hg-Co(CN)_5]^{6-}$.

Properties of $[(NC)_5Co-Hg-Co(CN)_5]^{6-}$

The proposed composition of the complex is supported by the stoichiometry of the reactions leading to its formation (Fig. 2). The same complex results if $Hg(ClO_4)_2$ rather than $Hg(CN)_2$ is treated with $Co(CN)_5H^{3-}$, showing that the cyanide ligands originally attached to Hg(II) are not essential for the complex to be formed. Addition of large excesses of chloride or bromide ions to the reaction mixture

Figure 1. -- Time dependence of the spectra of solutions containing $Co(CN)_5H^{3-}$ and $Hg(CN)_2$. The numbers on each curve are the time in minutes since the two reagents were mixed. The maximum absorbance at 274 nm was attained after 15 minutes. Initial conditions: $[Co(CN)_5H^{3-}] = 9 \times 10^{-5}$ M; $[Hg(CN)_2] = 1.5 \times 10^{-5}$ M; pH = 12; $[NaClO_4] = 1$ M.

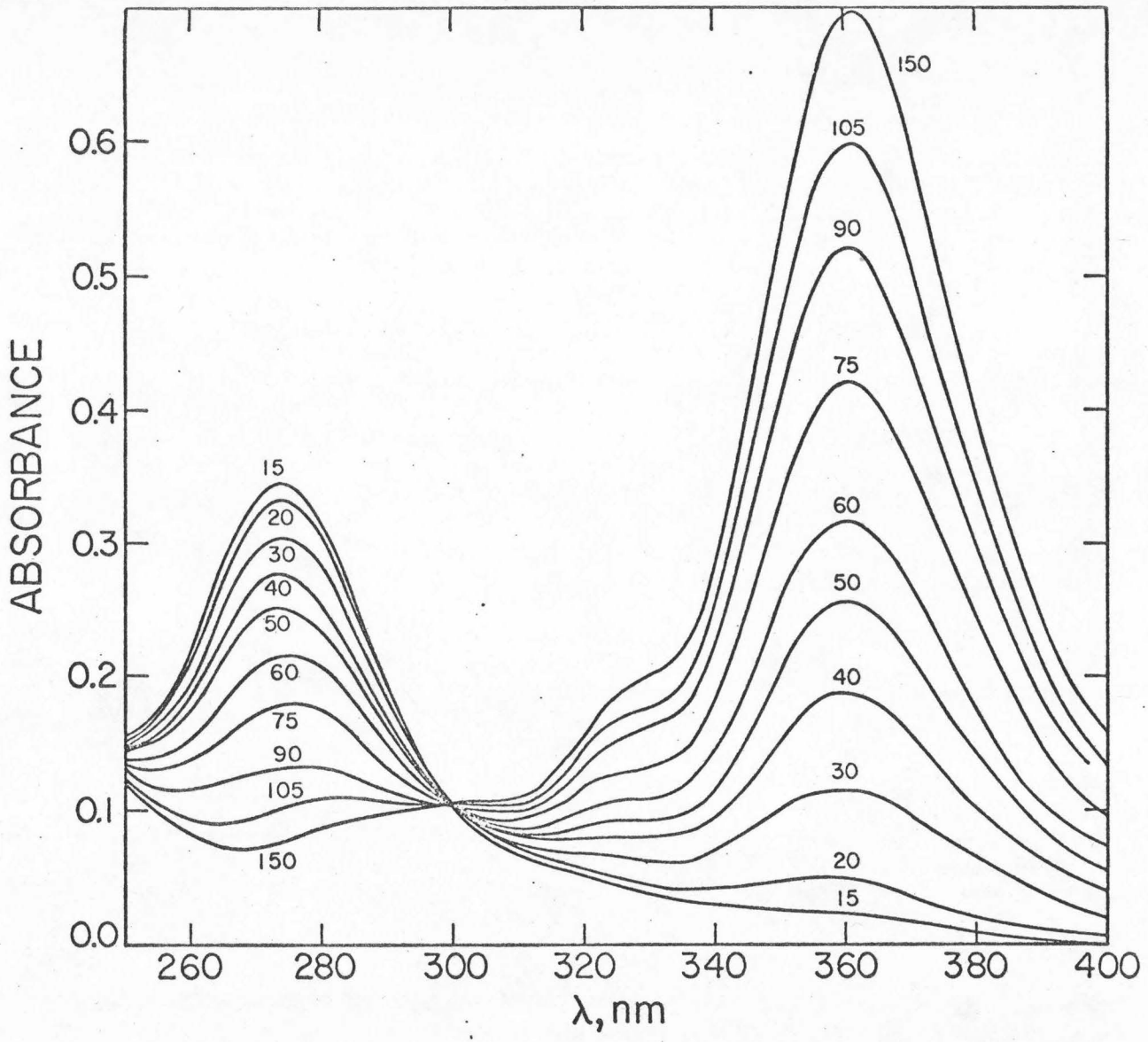
ABSORBANCE
0.0
0.1
0.2
0.3
0.4
0.5
0.6
260
280
300
320
340
360
380
400
λ, nm
150
105
90
75
60
50
40
30
20
15
15
20
30
40
50
60
75
90
105
150

Figure 2. -- Equilibrium absorbance of systematic mixtures of $Co(CN)_5H^{3-}$ and $Hg(CN)_2$ at 274 nm and 362 nm. The lines are calculated on the basis of the stoichiometry of reactions (1) and (2). The points are experimentally observed values. Initial conditions: $[Co(CN)_5H^{3-}] = 9 \times 10^{-5}$ M; $[NaClO_4] = [NaOH] = 0.5$ M.

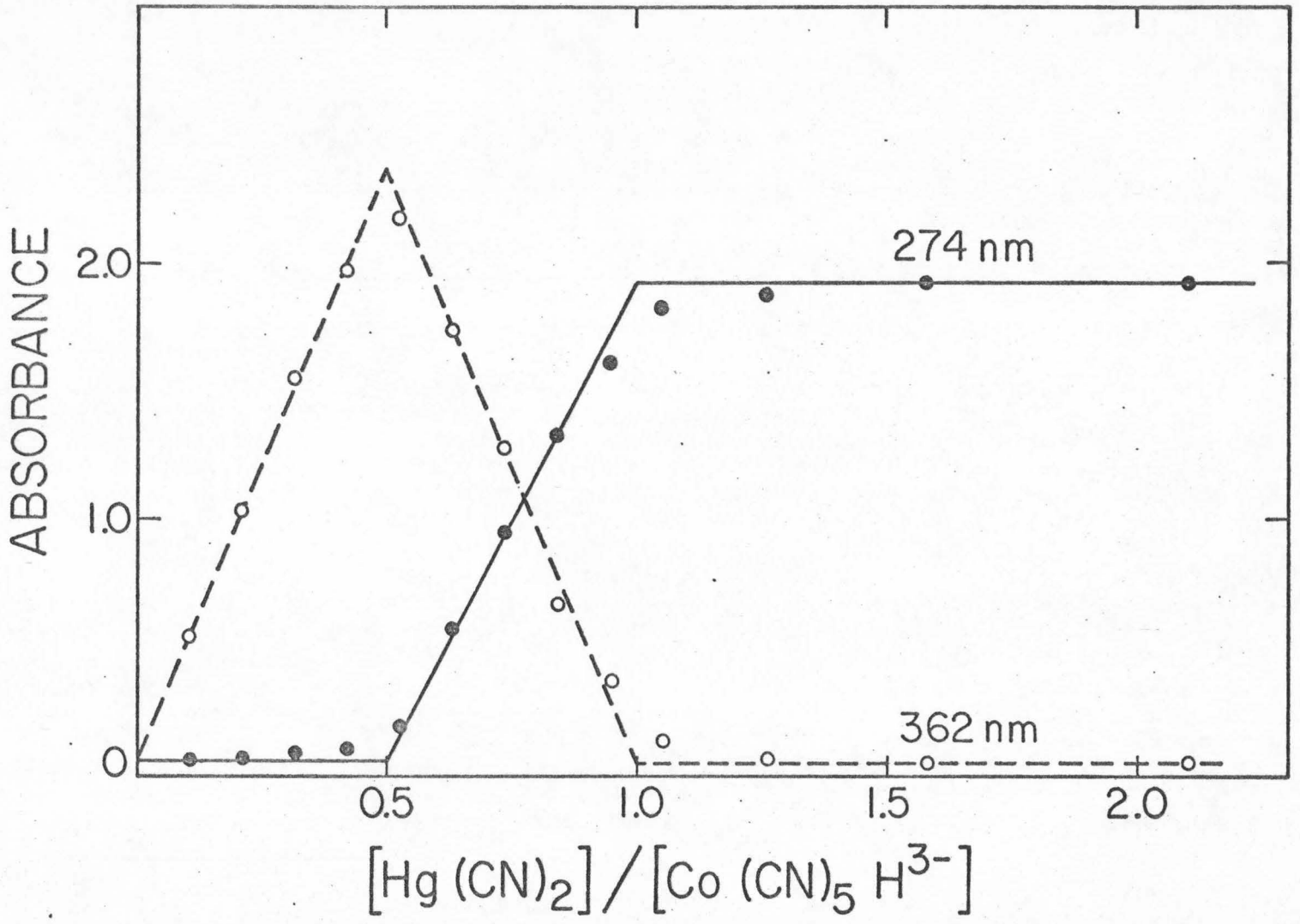
ABSORBANCE
2.0
1.0
0
274 nm
362 nm
0.5
1.0
1.5
2.0
[Hg (CN)2] / [Co (CN)5 H3-]

does not change the final spectrum obtained, indicating that no readily accessible coordination position is available on the Hg(II) ion once the two mercury-cobalt bonds are formed. The release of free cyanide as the complex is formed according to reactions (1) and (2) was confirmed polarographically. An anodic cyanide wave develops when $Hg(CN)_2$ is used to form the complex, but no corresponding wave appears when $Hg(ClO_4)_2$ is used. The magnetic susceptibility of the potassium salt of the complex ion was measured and showed the salt to be diamagnetic. These facts and the high value of the molar absorbance at 362 nm support the presence of the proposed metal-metal bonded configuration. Additional evidence is provided by the effect of lowering the temperature on the position of the absorption band. A solution of the complex in 10 M LiCl has its absorption maximum at 357 nm at 298°K and the band appears similar to that attributed to $\sigma \rightarrow \sigma^*$ transitions in carbonyl complexes containing metal-metal bonds.[5] This maximum is shifted to 347 nm when the temperature is lowered to 77°K. Such shifts to the blue at lower temperatures have been correlated with the presence of metal-metal bonding in several other complexes.[5]

The position and intensity of the absorption band obtained with the mercury(II) (and cadmium(II)) complexes are also nicely matched by those of two similar complexes which have been concluded to possess metal-metal bonds (Table I). A similar matching of bands occurs in the infrared in the cyanide stretch region. Table IIA compares the infrared spectra obtained with potassium salts of the

TABLE I

SPECTRAL PROPERTIES OF SOME METAL-BRIDGED COMPLEXES OF PENTACYANOCOBALTATE

Metal	λ_{max}, nm	ϵ, $cm^{-1}\underline{M}^{-1}$	Reference
Cd	348	ca. 30,000	a
Hg[b]	362	52,000	a
Tl(I)	389	57,000	6
$SnCl_2$	405	ca. 10,000	7

[a] This study.

[b] Other absorption maxima observed with this complex are as follows: $\epsilon_{325} \sim 11,000$ (shoulder); $\epsilon_{300} \sim 5,000$; $\epsilon_{230} \sim 12,000$ $cm^{-1}\ \underline{M}^{-1}$.

TABLE II

A

Infrared spectra of some cyanocobaltate complexes in the cyanide stretch region in KBr disk (in cm^{-1})		Reference
Potassium salt of $[HgCo_2(CN)_{10}]^{6-}$	2128 (s), 2099 (m), 2072 (s, br) ca. 2035 (w, sh)	a
Potassium salt of $[CdCo_2(CN)_{10}]^{6-}$	2128 (m), 2090 (m), 2062 (s, br), 2050 (sh)	a
$K_4H_2[Co_2(CN)_{10}] \cdot 4H_2O$ [b]	2127 (s), 2099 (m), 2077 (s, br) ca. 2040 (w, sh)	a
$K_6[Co_2(CN)_{10}]$	2133 (s), 2090 (s), 2079 (s)	9

B

Infrared spectra of manganese-carbonyl complexes in the carbonyl stretch region in KBr disk (in cm^{-1})		
$Hg[Mn_2(CO)_{10}]$	2067 (s), 2008 (s, sh), 1975 (vs)	10
$[Mn_2(CO)_{10}]$	2060 (m), 2014 (vs), 1989 (s)	10

where s = strong, m = medium, w = weak, vs = very strong, br = broad, and sh = shoulder.

[a] Data from this study.

[b] Prepared according to the procedure in reference 8.

mercury(II) and cadmium(II) complexes with those of two binuclear cobalt complexes known to contain cobalt-cobalt bonds. The close similarity of the cyanide stretching frequencies among these four complexes supports the structures proposed for the mercury(II) and cadmium(II) complexes. Further support results from the additional comparison (Table IIB) with the spectra of dimanganese decacarbonyl and its mercury derivative, which is known to contain two mercury-manganese bonds.[10]

The $[XHg-Co(CN)_5]^{3-}$ Complex

Efforts to isolate a salt of this complex anion (with X = CN or OH) were unsuccessful. Nevertheless, the evidence for its existence is strong. Mixtures of $Hg(CN)_2$ and $Co(CN)_3H^{3-}$ having mercury to cobalt ratios of 1.0 develop a strong absorption band at 274 nm which gradually increases in intensity until a final absorption is reached which is quite stable. If additional $Co(CN)_5H^{3-}$ is added, however, the band at 274 nm decreases in intensity as the new band, attributed to $[(NC)_5Co-Hg-Co(CN)_5]^{6-}$, develops at 362 nm (Figs. 1 and 2). The stoichiometry of the reaction leading to the species which absorbs at 274 nm is consistent with its being $[NCHg-Co(CN)_5]^{3-}$ and this configuration seems quite likely because of its similarity to the analogous isoelectronic carbonyl complexes $XHg-Mn(CO)_5$, where X = Cl, Br, and I.[10] Added evidence for the proposed structure of the complex is the fact that species giving very similar spectra in the region from 274-290 nm are also produced when $Co(CN)_5H^{3-}$ is treated

with equal or greater quantities of CH_3HgOH, C_6H_5HgOH, or $Hg(OH)_2$ (obtained by adding $Hg(ClO_4)_2$ to the alkaline reaction solution). The complex resulting from CH_3HgOH persists for some time even in the presence of excess $Co(CN)_5H^{3-}$ while with C_6H_5HgOH formation of $[(NC)_5CoHgCo(CN)_5]^{6-}$ occurs less slowly. (The fate of the methyl and phenyl groups during the second stage of these reactions was not investigated.) A number of closely analogous carbonyl complexes have been described.[11, 12]

Reaction of $Co(CN)_5^{3-}$ with $Hg(CN)_2$

Both $[NCHg-Co(CN)_5]^{3-}$ and $[(NC)_5Co-Hg-Co(CN)_5]^{6-}$ are also formed if $Co(CN)_5^{3-}$ and $Hg(CN)_2$ are allowed to react in alkaline solutions, but the rate of the reaction is much smaller than when $Co(CN)_5H^{3-}$ is used. The band due to $[NCHg-Co(CN)_5]^{3-}$ that develops at 274 nm is not as simple to follow because of the sizeable absorption of $Co(CN)_5^{3-}$ at this wavelength.[13] However, the band at 362 nm, due to $[(NC)_5Co-Hg-Co(CN)_5]^{6-}$, is readily observed and it reaches a maximum absorption when the ratio of reactants, $Hg(CN)_2/Co(CN)_5^{3-}$, is 0.2 or less. With ratios greater than 0.2, the absorption at 362 nm never achieves stability while with lower ratios, e.g., 0.1, the absorption at 362 nm remains at its maximum value for several days.

During the growth of the absorption at 362 nm the total absorption at 280 nm, where $Co(CN)_5^{3-}$ has an absorption maximum and where $[NCHgCo(CN)_5]^{3-}$ also absorbs strongly, decreases. When the absorption at 362 nm attains its maximum stable value, the

absorption at 280 nm is smaller than its initial value corresponding to the concentration of $Co(CN)_5^{3-}$ present before any reactions occurred. This decrease in absorption at 280 nm corresponds to the consumption of ca. 4 moles of $Co(CN)_5^{3-}$ for each mole of $Hg(CN)_2$ used.

These observations can be accommodated by the overall reaction

$$4\,Co(CN)_5^{3-} + Hg(CN)_2 + 2OH^- \longrightarrow$$

$$[(NC)_5Co-Hg-Co(CN)_5]^{6-} + 2\,Co(CN)_5OH^{3-} + 2\,CN^-. \quad (3)$$

It seems likely that the slower rate and different stoichiometry obtained with $Co(CN)_5^{3-}$ result because of the need for an initial disproportionation reaction[2, 14, 15]

$$2\,Co(CN)_5^{3-} + H_2O \longrightarrow Co(CN)_5H^{3-} + Co(CN)_5OH^{3-} \quad (4)$$

to generate the $Co(CN)_5H^{3-}$ which enters into the reaction scheme given by reactions (1) and (2). The much more complex kinetics which result when $Co(CN)_5^{3-}$ is employed caused us to concentrate our studies on cases where $Co(CN)_5H^{3-}$ was the reactant. It may, however, prove useful to know that the same products can result with either cobalt complex as a reactant, especially in electrochemical studies of cobalt-cyanide complexes at mercury electrodes.[1] One unsuccessful attempt was made to observe a reaction between metallic mercury and $Co(CN)_5^{3-}$. An 80-ml sample of a 1 m$\underline{M}$ $Co(CN)_5^{3-}$ solution (pH ~11) was stirred over a 12 cm^2 mercury pool. The spectrum of the resulting solution indicated that the characteristic absorption of $Co(CN)_5^{3-}$ at 280 nm had declined to ca. one half of its initial value

after thirty minutes while a new, rather weak band was formed at 360-380 nm. However, after 14 hours of reaction the extinction at 362 nm corresponded to less than 1% of the $Co(CN)_5^{3-}$ having been converted to $[(NC)_5Co-Hg-Co(CN)_5]^{6-}$. This system was not investigated further.

Cadmium(II) is able to take the role of mercury(II) in the reaction with $Co(CN)_5H^{3-}$. The infrared and ultraviolet spectrum of the resulting complex is very similar to that of the mercury(II) complex (Tables I and IIA).

Kinetics of the Reaction between $Co(CN)_5H^{3-}$ and $Hg(CN)_2$

The stoichiometry of the first stage of the reaction between $Co(CN)_5H^{3-}$ and $Hg(CN)_2$ is as shown in reaction (1). The rate of the reaction is low enough to be conveniently followed spectrophotometrically at pH values between 11 and 12 if the reactant concentrations are in the range $10^{-5} - 10^{-4}$ M. The formation of $[NCHg-Co(CN)_5]^{3-}$ proceeds considerably faster than does its subsequent conversion to $[(NC)_5Co-Hg-Co(CN)_5]^{6-}$ so that the first stage of the reaction can be followed by monitoring the absorbance at 274 nm before significant consumption of the binuclear complex occurs. Kinetic runs were carried out with comparable concentrations of $Co(CN)_5H^{3-}$ and $Hg(CN)_2$ but with a much larger and therefore essentially constant concentration of hydroxide ion. Analysis of the resulting rate data according to the simple second-order kinetic equation[16] showed that they deviated significantly from simple second-order kinetics in that the

calculated rate constant displayed a systematic dependence upon the initial concentration of mercuric cyanide, Table III. The deviations were in the direction to be expected if the rate-determining step were preceded by quasi-reversible formation of a reactive intermediate. A likely mechanism for the reaction suggested by these results is the following:

$$Co(CN)_5H^{3-} + OH^- \underset{k_{-1}}{\overset{k_1}{\rightleftharpoons}} Co(CN)_5^{4-} + H_2O \qquad (5)$$

$$Co(CN)_5^{4-} + Hg(CN)_2 \xrightarrow{k_2} [NCHg\text{–}Co(CN)_5]^{3-} + CN^- \qquad (6)$$

where $Co(CN)_5^{4-}$ is the reactive intermediate and reaction (6) is irreversible. Applying the steady-state approximation[17] to the concentration of $Co(CN)_5^{4-}$ leads to the following rate equation:

$$\frac{dP}{dt} = \frac{k_2 k_1 [OH^-][Co(CN)_5H^{3-}][Hg(CN)_2]}{k_{-1} + k_2[Hg(CN)_2]} \qquad (7)$$

where P is the concentration of the product of the reaction, $[NCHg\text{–}Co(CN)_5]^{3-}$. Integration of equation (7) leads to

$$\frac{1}{A-B} \ln\left[\frac{B(A-P)}{A(B-P)}\right] + \frac{k_2}{k_{-1}} \ln\left[\frac{A}{A-P}\right] = \frac{k_2 k_1}{k_{-1}} [OH^-]t \qquad (8)$$

where A and B are the initial concentrations of $Co(CN)_5H^{3-}$ and $Hg(CN)_2$, respectively. When equation (8) was used to analyze the rate data, the apparent dependence of the rate constant on the initial concentration of $Hg(CN)_2$ (Table III) disappeared, Fig. 3.

TABLE III

KINETIC DATA ANALYZED ACCORDING TO THE SIMPLE SECOND ORDER RATE EQUATION: $\frac{d[\text{product}]}{dt} = k'[OH^-][Co(CN)_5H^{3-}][Hg(CN)_2]$ WITH $[OH^-]$ = constant.

pH	Initial concentrations, $Co(CN)_5H^{3-}$ M $\times 10^5$	$Hg(CN)_2$	k', $M^{-2}\ sec^{-1}$ $\times 10^{-3}$
11.40	18.8	1.0	2.24
11.40	18.8	2.0	1.96
11.44	18.8	5.0	1.23
11.44	18.8	10	0.745
11.34	9.4	5.0	1.18
11.64	3.76	5.0	1.12
11.27	9.4	4.0	1.23

Figure 3. -- Kinetic data analyzed according to equation (8). The solid line, calculated by least-squares fitting of the data, corresponds to $\frac{k_2}{k_{-1}} = (2.18 \pm 0.11) \times 10^4$ $\underline{M}^{-1}$ and $\frac{k_2 k_1}{k_{-1}} = (2.12 \pm 0.03) \times 10^3$ sec^{-1} $\underline{M}^{-1}$. The plotted points correspond to initial $Hg(CN)_2$ concentrations of: ■ -- 10^{-5} $\underline{M}$; □ -- 2×10^{-5} $\underline{M}$; ● -- 4×10^{-5} $\underline{M}$; ○ -- 5×10^{-5} $\underline{M}$; ▲ -- 10^{-4} $\underline{M}$. The initial concentrations of $Co(CN)_5H^{3-}$ were in the range 4-19 $\times 10^{-5}$ $\underline{M}$ and the pH was between 11.3 and 12.1; $\mu = 0.5$ ($NaClO_4$); T = 24.0°C.

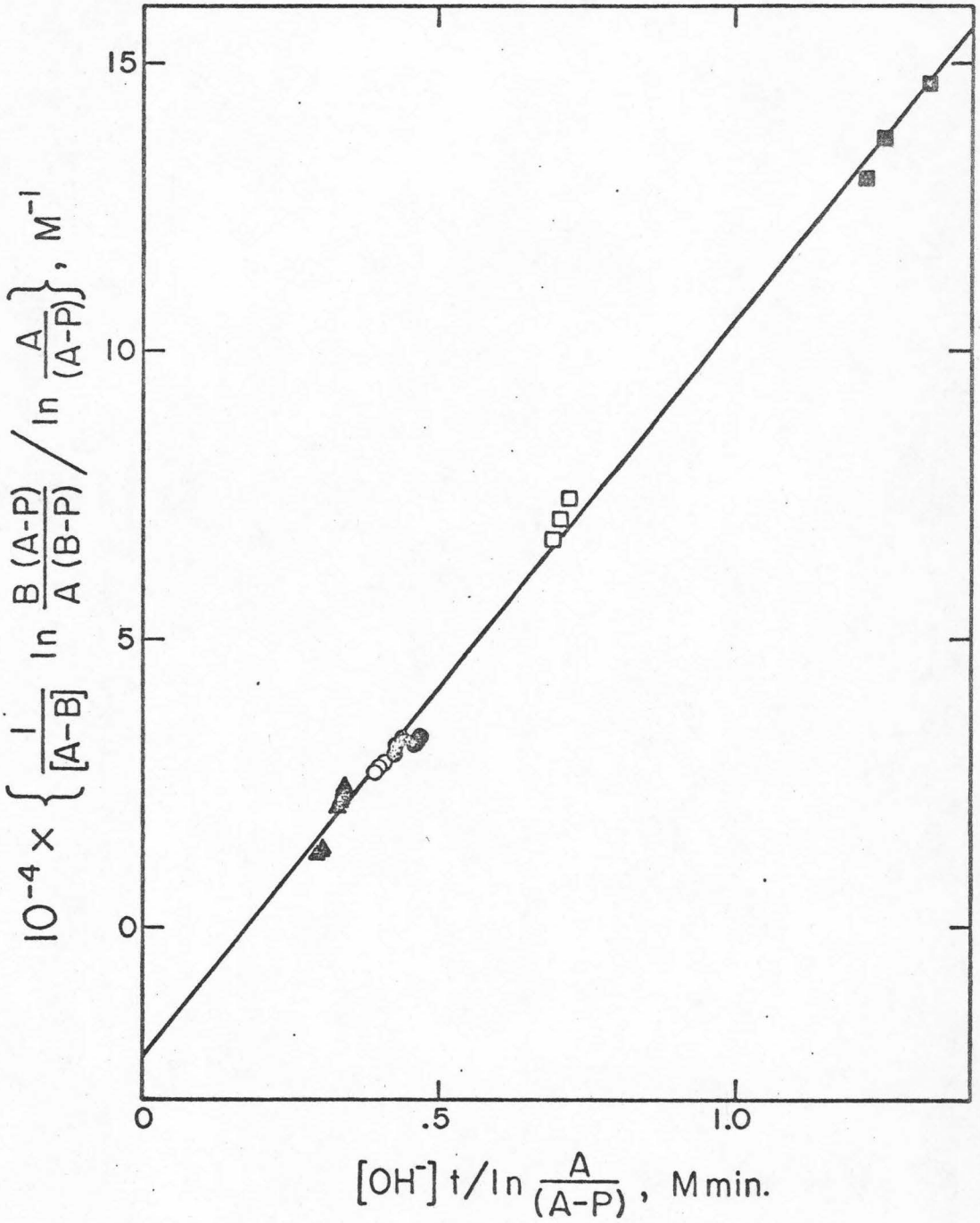
15
10
5
0
0
.5
1.0
$10^{-4} \times \left\{ \frac{1}{[A-B]} \ln \frac{B(A-P)}{A(B-P)} \Big/ \ln \frac{A}{(A-P)} \right\}$, M^{-1}
$[OH^-]\, t / \ln \frac{A}{(A-P)}$, M min.

The order of the reaction with respect to hydroxide was determined by measuring the rate under second-order conditions at a series of constant concentrations of hydroxide ion. The results, plotted in Fig. 4, confirm a first-order hydroxide dependence.

The slope and intercept of the least-squares line shown in Fig. 3 yield the following values of the kinetic parameters: $\frac{k_2}{k_{-1}} = (2.18 \pm 0.11) \times 10^4$ $\underline{M}^{-1}$ and $\frac{k_2 k_1}{k_{-1}} = k_2 K = (2.12 \pm 0.03) \times 10^3$ $\sec^{-1}$ $\underline{M}^{-2}$, where K is the equilibrium constant for reaction (5).

Equation (7) predicts that the reaction rate should become zero order with respect to the concentration of $Hg(CN)_2$ when $k_{-1} \ll k_2[Hg(CN)_2]$. The value of $\frac{k_2}{k_{-1}}$ obtained from the kinetic data is 2.2×10^4 $\underline{M}^{-1}$ so that the necessary condition for apparent zero-order dependence on $Hg(CN)_2$ becomes $[Hg(CN)_2] \gg 4.6 \times 10^{-5}$ $\underline{M}$. To test this prediction, kinetic runs were carried out with much larger concentrations of $Hg(CN)_2$. Under these conditions, the reaction became pseudo-first order and the first order rate constants obtained at various concentrations of $Hg(CN)_2$ are summarized in Table IV. Contrary to the expectations based on equation (7), the reaction rate continues to depend upon the concentration of $Hg(CN)_2$ up to concentrations of $Hg(CN)_2$ as high as 0.1 $\underline{M}$. It follows that equation (7) does not give an adequate account of the observed kinetics at high concentrations of $Hg(CN)_2$. To explain the observed behavior, a second reaction pathway leading to the same product is needed. A good possibility[18] is

Figure 4. -- pH Dependence of the the reaction rate. Initial concentrations: $Co(CN)_5H^{3-} = 9 \times 10^{-5}$ M; $Hg(CN)_2 = 4 \times 10^{-5}$ M; $\mu = 0.5$ ($NaClO_4$); T = 24°C. The ordinate values were obtained from analysis according to equation (8) with $\frac{k_2}{k_{-1}}$ set equal to 2.18×10^4 M^{-1}.

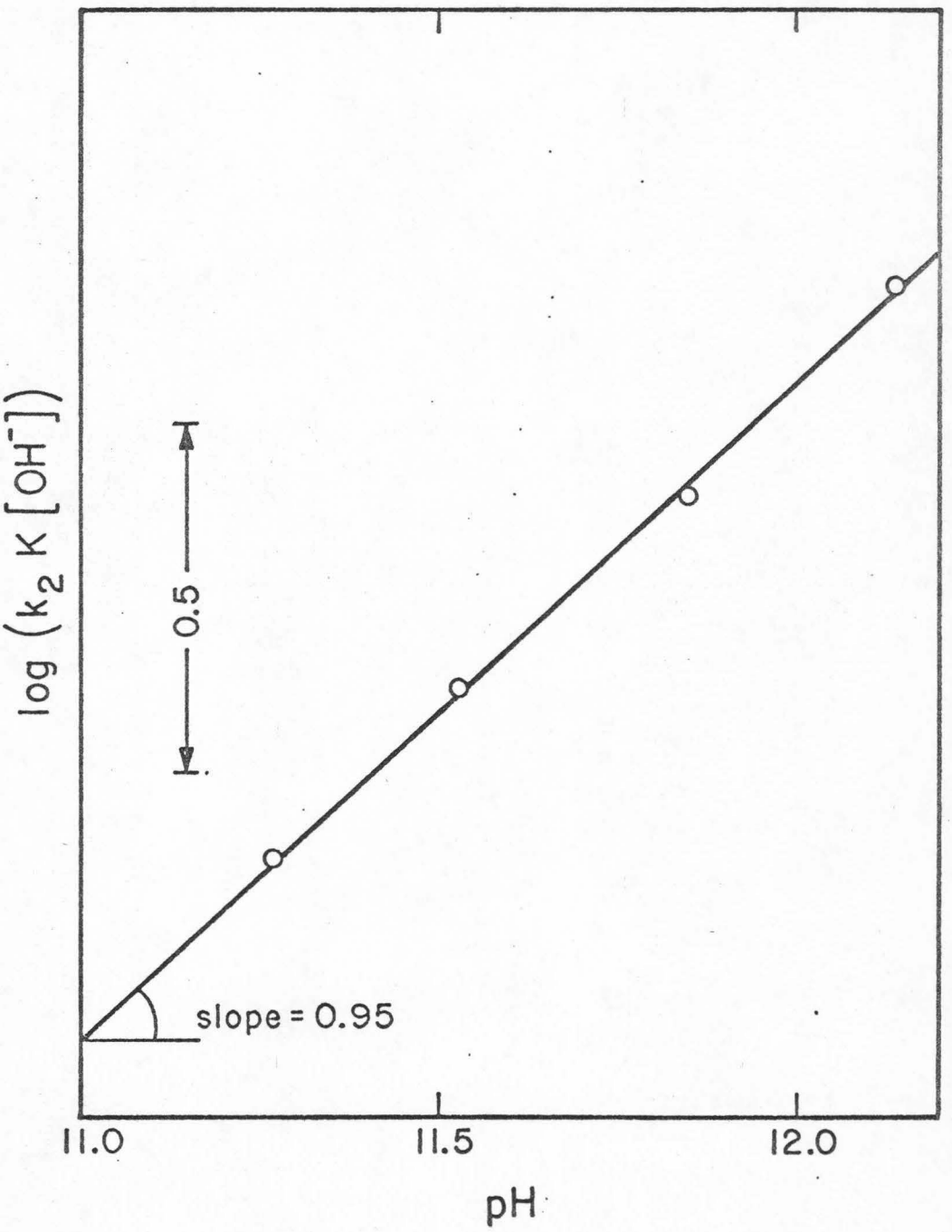
log (k_2 K [OH^-])
0.5
slope = 0.95
11.0
11.5
12.0
pH

TABLE IV

FIRST ORDER RATE CONSTANTS OBTAINED AT HIGH CONCENTRATIONS OF $Hg(CN)_2$.

Initial concentrations,[a] mM		$\frac{[Hg(CN)_2]}{[OH^-]}$	$\frac{k_{obs}}{[OH^-]}$; $M^{-1}\,sec^{-1} \times 10^1$
$Hg(CN)_2$	OH^-		
4.0	5.76	0.695	1.06 ± 0.003
10	6.16	1.62	1.10 ± 0.005
40	5.76	6.95	1.66 ± 0.007
70	5.37	13.05	2.24 ± 0.010
100	5.01	19.95	2.96 ± 0.015

[a] The initial concentration of $Co(CN)_5H^{3-}$ was 9.8×10^{-5} M in each case.

$$Co(CN)_5H^{3-} + Hg(CN)_2 \xrightarrow{k_3} [NCHg-Co(CN)_5]^{3-} + HCN \qquad (9)$$

in which the hydrido complex reacts directly with $Hg(CN)_2$. Hanzlik and Vlček have proposed an analogous direct reaction of $Co(CN)_5H^{3-}$ with benzoquinone.[19]

If the parallel reaction pathway indicated by reaction (9) is considered along with reactions (5) and (6) the rate law becomes

$$\frac{dP}{dt} = [Co(CN)_5H^{3-}][Hg(CN)_2] \frac{k_1 k_2 [OH]}{k_{-1} + k_2[Hg(CN)_2]} + k_3 \quad . \qquad (10)$$

For all of the cases listed in Table IV the condition $[Hg(CN)_2] \gg 4.6 \times 10^{-5}$ M is met, so that equation (10) simplifies to

$$\frac{dP}{dt} = \left(k_1 + k_2 \frac{[Hg(CN)_2]}{[OH^-]} \right) [OH^-][Co(CN)_5H^{3-}]. \qquad (11)$$

Pseudo-first order rate constants, k_{obs}, were evaluated and divided by $[OH^-]$. Table IV lists the resulting values of $k_{obs}/[OH^-]$, which can be identified with the first term in equation (11)

$$\frac{k_{obs}}{[OH^-]} = k_1 + k_3 \frac{[Hg(CN)_2]}{[OH^-]} \qquad (12)$$

Plots of $k_{obs}/[OH^-]$ versus $[Hg(CN)_2]/[OH^-]$ were linear and produced the following values for the rate constants: $k_1 = (9.6 \pm 0.2) \times 10^{-2}$ M^{-1} sec^{-1} and $k_3 = (9.9 \pm 0.2) \times 10^{-3}$ M^{-1} sec^{-1}. This value of k_1 agrees well with the value obtained from the ratio of the slope to the intercept of the line in Fig. 3 ($k_1 = (9.7 \pm 0.8) \times 10^{-2}$ M^{-1} sec^{-1}).

The value of k_3 is small enough to assure that reaction (9) made no significant contribution to the kinetics observed with the lower concentrations of $Hg(CN)_2$ employed in the experiments used to obtain the kinetic parameters from Fig. 3.

Free Cyanide Ion Dependence

A few kinetic runs were performed in solutions to which more than 5 cyanide ions per cobalt(II) ion were added. The rate of reaction was decreased by free cyanide in the way to be expected if $Hg(CN)_2$ were much more reactive than $Hg(CN)_4^=$ and somewhat more reactive than $Hg(CN)_3^-$. A more quantitative evaluation was not attempted because of the uncertainties in the reported values of the mercury(II)-cyanide complex equilibrium constants.

Comparison with Other Results

The value of k_1 resulting from this study is $k_1 = (9.6 \pm 0.8) \times 10^{-2}$ $\underline{M}^{-1}$ sec^{-1} at 24°C. Recent pulse radiolysis experiments gave a value of 10^{+5} sec^{-1} for k_{-1}.[20] The equilibrium constant for reaction (5) is therefore calculated to be $K = 1 \times 10^{-6}$ $\underline{M}^{-1}$. Hanzlik and Vlček have estimated this constant to be ca. 10^{-4} $\underline{M}^{-1}$ on the basis of unpublished polarographic data[19] but the experimental data they cite cannot be used to estimate this constant unless a value for the standard potential of reaction (13) is known.

$$Co(CN)_5^{3-} + e^- = Co(CN)_5^{4-}. \qquad (13)$$

In strongly alkaline solutions of $Co(CN)_5H^{3-}$ an anodic polarographic wave[21] commencing at 1.2 V vs. S.C.E. has been attributed to the reverse of reaction (13) but the thermodynamic reversibility of the wave has not been established. If the known equilibrium constant for

$$2\,Co(CN)_5^{3-} + H_2 = 2\,Co(CN)_5H^{3-} \qquad K = 1.53 \times 10^5\ \underline{M}^{-1}\ ^{15} \qquad (14)$$

is combined with the ionization constant of water and the calculated value of $K = 10^{-6}\ \underline{M}^{-1}$ for reaction (5), the standard potential for reaction (13) is calculated to be -1.27 V vs. S.C.E. This value is not incompatible with the meager polarographic data presently available.[21]

Combining the value of k_2/k_{-1} obtained from Fig. 3 with the pulse radiolysis value[20] of $k_{-1} = 10^5\ sec^{-1}$ yields $k_2 = 2 \times 10^9\ \underline{M}^{-1}\ sec^{-1}$, a value reflecting the high reactivity of $Co(CN)_5^{4-}$ as pointed out by Hanzlik and Vlček.[19] These authors estimated a minimum value for the second-order rate constant for the reaction between $Co(CN)_5^{4-}$ and p-benzoquinone to be ca. $10^9\ \underline{M}^{-1}\ sec^{-1}$ at 0°C. This constant increases to $10^{11}\ \underline{M}^{-1}$ if the equilibrium constant for reaction (5) obtained from this study ($K = 10^{-6}\ \underline{M}^{-1}$) is substituted for the estimated value ($K = 10^{-4}\ \underline{M}^{-1}$) used by Hanzlik and Vlček.[19] This value for the rate constant is uncomfortably large and it seems likely that Hanzlik and Vlček's assumption that reaction (5) proceeded rapidly enough to maintain equilibrium during their measurements caused them to derive an erroneously large rate constant from their data. The value of k_{-1} reported by Venerable, Hart, and Halpern[20]

is too low by a factor of $10^2 - 10^3$ to permit the assumption of fast equilibrium for reaction (5) when the $Co(CN)_5^{4-}$ being generated is exposed to substrates with which it reacts as rapidly as it does with benzoquinone or mercuric cyanide.

REFERENCES

1. H. S. Lim and F. C. Anson, Part II of present report.
2. N. K. King and M. E. Winfield, J. Amer. Chem. Soc., 83, 3366 (1961).
3. R. Grassi, A. Haim, and W. K. Wilmarth, Inorg. Chem., 6, 237 (1967).
4. I. M. Kolthoff and R. Belcher, "Volumetric Analysis", Vol. III, Interscience, New York, N. Y., 1957, pp. 451-469.
5. R. A. Levenson, Thesis, Columbia University, 1970; R. A. Levenson and H. B. Gray, to be published.
6. E. C. C. Crouch and J. M. Pratt, J. Chem. Soc. (D), 1243 (1969).
7. A. A. Vlček and F. Basolo, Inorg. Chem., 5, 156 (1966).
8. R. Nast, H. Ruppert-Mesche, and M. Helbig-Neubauer, Z. Anorg. Allg. Chem., 312, 314 (1961).
9. W. P. Griffith and G. Wilkinson, J. Inorg. Nucl. Chem., 7, 295 (1958).
10. W. Hieber and W. Schropp, Jr., Chem. Ber., 93, 455 (1960).
11. M. C. Baird, in "Progress in Inorganic Chemistry", Vol. 9, F. A. Cotton, Ed., Interscience, New York, N. Y., 1968, pp. 1-159.
12. W. Jehn, Z. Chem., 9, 170 (1969).
13. J. J. Alexander and H. B. Gray, J. Amer. Chem. Soc., 89, 3356 (1967).
14. B. DeVries, J. Catalysis, 1, 489 (1962).

15. M. G. Burnett, P. J. Connolly, and C. Kemball, J. Chem. Soc. (A), 800 (1967).

16. A. A. Frost and R. G. Pearson, "Kinetics and Mechanism", John Wiley & Sons, Inc., New York, N. Y., 1953, p. 15.

17. Reference 16, p. 179.

18. J. Halpern and L. Y. Wong, J. Amer. Chem. Soc., 90, 6665 (1968).

19. J. Hanzlik and A. A. Vlček, Inorg. Chem., 8, 669 (1969).

20. G. D. Venerable II, E. J. Hart, and J. Halpern, J. Amer. Chem. Soc., 91, 7538 (1969).

21. J. Hanzlik and A. A. Vlček, Chem. Commun., 47 (1969).

Part II. Electrochemical Behavior of Pentacyanocobaltate(II) and Substituted Pentacyanocobaltate(III) Complexes at Mercury Electrodes

Part II is in press in J. Electroanal. Chem.

ELECTROCHEMICAL BEHAVIOR OF PENTACYANOCOBALTATE(II) AND SUBSTITUTED PENTACYANOCOBALTATE(III) COMPLEXES AT MERCURY ELECTRODES

Previous electrochemical studies of $Co(CN)_5^{3-}$ and $Co(CN)_5X^{3-}$ ($X = Cl^-$, Br^-, I^-, N_3^-, NCS^-, H_2O, CN^-) have been largely confined to conventional polarographic measurements with dropping mercury electrodes.[1-4] As part of a study of ligand bridging by adsorbed anions during the electrochemical oxidation of $Co(CN)_5^{3-}$ at hanging mercury drop electrodes, we examined the cathodic reduction of a number of cobalt(III) complexes which might result from oxidation of $Co(CN)_5^{3-}$. At the outset we observed a strong dependence of the electrochemical behavior upon the length of time the mercury electrode was exposed to solutions of $Co(CN)_5^{3-}$ or $Co(CN)_5X^{3-}$. This feature of the electrochemistry had not been encountered in previous studies because of the relatively brief exposure of the electrode to the solutions that obtain in conventional polarographic experiments (typically 3-5 sec). With longer exposure times very prominent and sharp "adsorption peaks" appear in the current-potential curves obtained in linear potential-scan experiments. We have examined the behavior of these adsorption peaks in considerable detail to try to establish the

identity of the adsorbing species and the reasons for the adsorption peak's developing as slowly as it does. Our conclusions are that the same species, probably a tetracyanocobaltate(II) complex, is the adsorbed species responsible for the peak regardless of whether the complex in the bulk of the solution is $Co(CN)_5^{3-}$ or $Co(CN)_5X^{3-}$. The reduction of the adsorbed complex to a cobalt(I) intermediate appears to be followed by a series of rapid reactions which lead to the consumption of two additional electrons with the likely formation of a bishydrido cobalt complex. This sequence of electrode and chemical reactions is responsible for the magnitude and sharpness of the adsorption waves. The experimental evidence upon which these conclusions are based forms the basis for this report.

EXPERIMENTAL

Reagents

Most of the cobalt(III) complexes were prepared according to published procedures: $K_3Co(CN)_5Cl$ [5], $K_3Co(CN)_5Br$ [6], $K_3Co(CN)_5I$ [7], $K_3Co(CN)_5N_3$ [8], $K_3Co(CN)_5SCN$ [9], $K_3Co(CN)_6$ [10]. A sample of $K_3Co(CN)_5NCS$ was kindly supplied by Gutterman and Gray who have described its synthesis [11]. Stock solutions containing 1-2 mM $Co(CN)_5H_2O^{2-}$ were prepared by reacting stoichiometric quantities of $K_3Co(CN)_5N_3$ and HNO_2 [8] and stored at pH 6. These solutions were discarded within two weeks of their preparation. Solutions of

$Co(CN)_5H^{3-}$ were prepared by controlled potential reduction of $Co(CN)_5Cl^{3-}$ or $Co(CN)_5^{3-}$ at a mercury pool at -1500 to -1600 mV vs. S. C. E.. Solutions of $Co(CN)_5^{3-}$ were prepared by mixing, with hypodermic syringes in the absence of air, stoichiometric quantities of $Co(NO_3)_2$ and NaCN in appropriate supporting electrolytes just before the resulting solution was to be used. These solutions were examined for purity by comparison of their spectra with published spectra[12]. Stock solutions of 8 F $NaClO_4$ were prepared from $HClO_4$ and Na_2CO_3 as described previously[13]. Triply distilled water was used to prepare all solutions. Prepurified nitrogen gas used to deaerate solutions was further purified by consecutive passage through vanadium(II) and chromium(II) solutions or through copper turnings maintained at 400°C in a furnace.

Apparatus

The electronic apparatus employed for the cyclic voltammetric and chronocoulometric experiments has been described[14,15] as has the computerized data acquisition system which was utilized in some of the experiments[16]. Conventional two compartment cells were employed with commercially available Metrohm-type hanging mercury drop electrodes.

Potentials were measured and are reported with respect to a calomel electrode saturated with NaCl which had a potential 5-6 mV more negative than a S. C. E.

Conventional d. m. e. polarograms were obtained with a polarograph consisting of appropriately interconnected operational amplifiers (Philbrick Type P-65 and P-75). Slow potential scans (1-2 mV/sec) were obtained from a motor driven potentiometer and current-potential curves were read out on an X-Y Recorder.

Ultraviolet and visible spectra were recorded on a Cary Model 14 Spectrophotometer or measured manually on a Beckman Model DU Spectrophotometer attached to a Gilford Absorbance Indicator, Model 220.

Experiments were carried out at room temperature (22-26°C) unless otherwise noted.

Procedures

Because of the significant dependence of the observed behavior on the length of time the hanging mercury drop electrode was exposed to the solution, a standardized procedure was adopted for commencing each experiment: Each new mercury drop electrode was exposed to the test solution for 60 seconds while the solution was being stirred followed by 20 seconds without stirring. Tests showed that changes resulting from longer exposure times produced only minor additional changes in the resulting cyclic voltammograms.

Chronocoulometric data were obtained and analyzed with the computerized apparatus according to previously described procedures[16]. Usually 100 data points were taken at one millisecond intervals and stored in the memory of the computer. The data

were then analyzed by least-squares fitting to the usual chronocoulometric equations [17, 18].

RESULTS

Cyclic Voltammetry

The major electrochemical characteristics displayed by all the complexes of the class $Co(CN)_5X^{3-}$, where $X^- = I^-$, Br^-, Cl^-, N_3^-, NCS^-, H_2O, CN^-, and N_3^-, were surveyed by means of cyclic voltammetric experiments. In unbuffered solutions of sodium perchlorate having pH values from 4 to 10 most of these cobalt(III) complexes yield two irreversible reduction waves separated by an extremely sharp current peak apparently arising from the reaction of an adsorbed species. Figure 1A contains a typical voltammogram for a single cycle of the potential. The first wave, I, can be identified with reaction (1) on the basis of the published polarographic data for the same complexes [1-3]

$$Co(CN)_5X^{3-} + e^- \longrightarrow Co(CN)_5^{3-} + X^- . \qquad (1)$$

The potential at which wave I appears depends upon the identity of X^- and the wave is shifted outside the accessible potential range in the cases $X^- = CN^-$ or H^-. The other normally shaped wave in Fig. 1, wave III, occurs at the same potential for almost all the cobalt(III) complexes. (The exceptions are the complexes in which $X^- = N_3^-$, OH^- and NCS^- where the first wave, I, does not occur prior

FIG. 1.

A -- Cyclic voltammogram for 1 mM $Co(CN)_5I^{3-}$ at pH 8, unbuffered in 1 F $NaClO_4$.

Initial potential = -300 mV.

Electrode exposure time was ca. 4 sec.

Potential scan rate = 10 V/sec.

Electrode area = 0.032 cm^2.

B -- As in A except exposure time was 60 sec with stirring followed by 20 sec without.

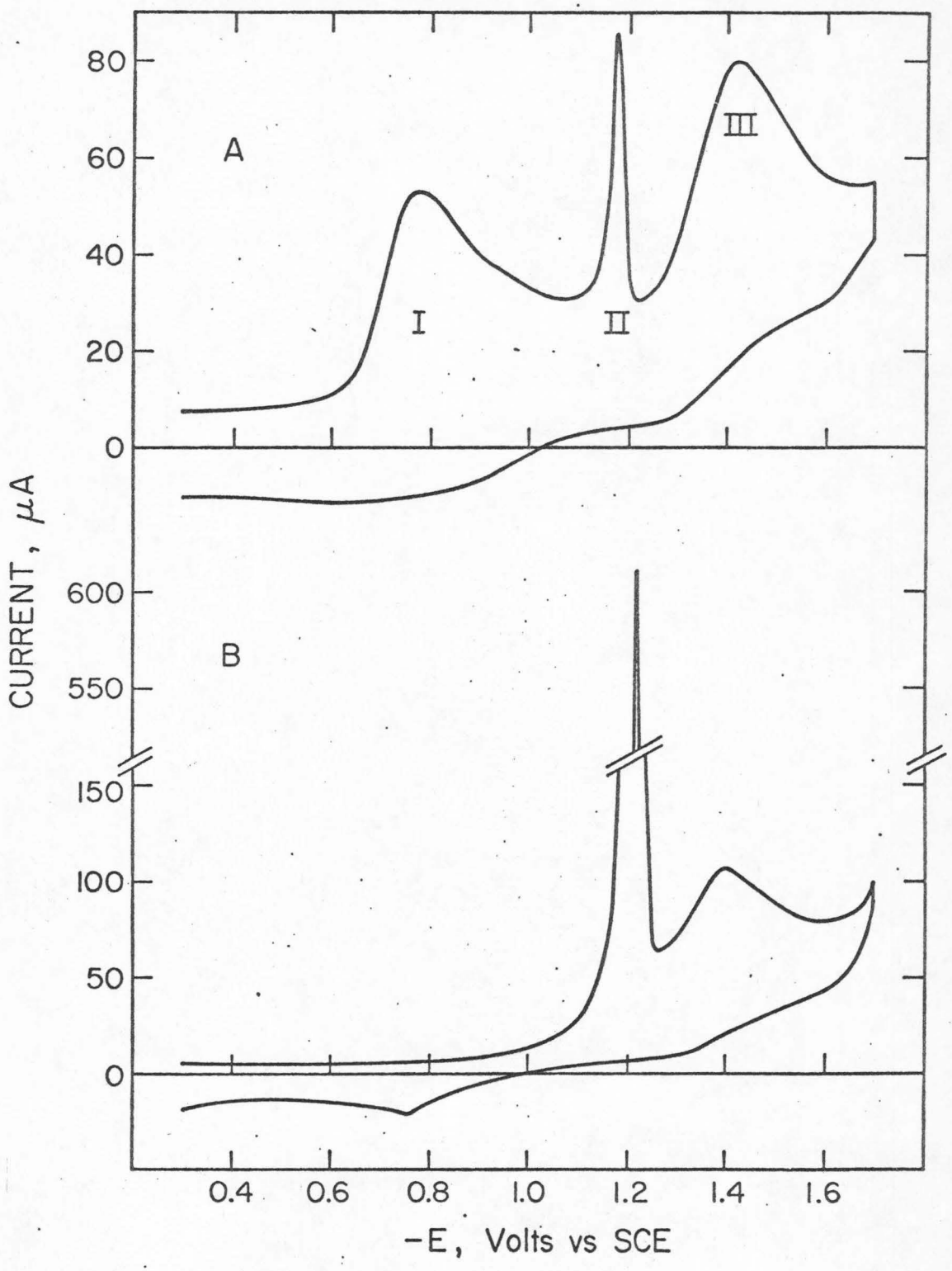
80
60
40
20
0
A
I
II
III
600
550
150
100
50
0
B
CURRENT, μA
0.4
0.6
0.8
1.0
1.2
1.4
1.6
-E, Volts vs SCE

to wave III so that a single 2-electron wave is observed.) The potential of wave III matches that of the single cathodic wave obtained in solutions of $Co(CN)_5^{3-}$. With the aid of previous polarographic data[1,4] it can be attributed to reaction (2). The cobalt(I) complex produced at the electrode by reaction (2)

$$Co(CN)_5^{3-} + e^- \longrightarrow Co(CN)_5^{4-} \qquad (2)$$

undergoes a fast follow-up chemical reaction to produce the electrochemically inert hydrido complex[1,2] as indicated in reaction (3)

$$Co(CN)_5^{4-} + H_2O = HCo(CN)_5^{3-} + OH^-. \qquad (3)$$

Controlled potential reduction of solutions of $Co(CN)_5X^{3-}$ or $Co(CN)_5^{3-}$ at potentials more negative than wave III, e.g., -1500 mV, leads to solutions whose spectra agree with the known spectra of the $Co(CN)_5H^{3-}$ ion[19] and the expected increases in pH are observed if unbuffered supporting electrolytes are employed.

The sharp peak labeled II in Fig. 1A has the appearance of an adsorption wave. When the hanging mercury drop electrode is exposed to the solution for 60 seconds or longer this peak attains its maximum height, as shown in Fig. 1B. The remarkable size and sharpness of this adsorption wave lead us to concentrate on it; to try to identify the adsorbed species giving rise to the wave and to determine the electrode reactions responsible for the sudden surge of current. Note also in Fig. 1B that wave I, which corresponds to the reduction of $Co(CN)_3I^{3-}$ to $Co(CN)_5^{3-}$, virtually disappears when

the exposure time is great enough for the full development of the adsorption peak. This aspect of the electrochemical behavior will be taken up later when the effects of the adsorption on the kinetics of the electrode reactions of unadsorbed species are considered.

For all of the complexes which give adsorption peaks, the peak potential appears at ca. -1150 mV. This potential remained within 50 mV of this value for exposure times from 10-100 seconds and sweep rates up to 40 V/sec. By contrast, the peak potential for the first wave (I in Fig. 1A) varied considerably from complex to complex and displayed a larger dependence on sweep rate. This constancy of the adsorption peak potential and the fact that the magnitude of the peak decreased sharply for all complexes at exposure potentials of -1000 mV suggest that a common adsorbing species is obtained with all the complexes and that it is desorbed in the vicinity of -1000 mV.

Additional adsorption peaks were sometimes obtained with certain complexes under special conditions but they were always less prominent and did not exhibit the constant potential typical of the adsorption peak in Fig. 1. We restricted our attention to this single, prominent adsorption peak and usually operated under conditions where it was the only adsorption peak present.

The magnitude of the adsorption peak currents obtained in the cyclic voltammetric experiments is a sensitive function of the potential of the electrode during its exposure to the solution prior to the recording of the current-potential curves. For some complexes the adsorption wave can be completely eliminated by keeping the

electrode at sufficiently anodic or sufficiently cathodic potentials. The behavior observed is summarized in Fig. 2 which shows how the adsorption peak current varies with the initial exposure potential for a series of complexes. The most important feature to note about the curves in Fig. 2 is that the adsorption peaks commence to appear at more positive potentials for just those cobalt(III) complexes which are reduced to $Co(CN)_5^{3-}$ at the more positive potentials. Thus, for example, wave I (Fig. 1) for $Co(CN)_5I^{3-}$ occurs at ca. -570 mV, the most positive reduction potential of all the complexes studied, and this complex shows a large adsorption peak at all exposure potentials from -200 to -900 mV. On the other hand, wave I for the $Co(CN)_5H_2O^{2-}$ complex comes at ca. -800 mV and this complex shows no adsorption peak at exposure potentials more positive than -500 mV vs. SCE. The same trend is evident with the other complexes and it implicates the reduction of the cobalt(III) complexes in the processes leading to the development of the adsorption peak, although it will be necessary to face the question of how the cobalt(III) complexes can be reduced at exposure potentials much more positive than the peak potential of the corresponding first wave (I in Fig. 1) of the cyclic voltammograms.

The magnitude of the adsorption peaks is also affected by the pH of the supporting electrolyte. The general trend is for the adsorption to decrease as the pH increases, with the peaks disappearing completely at pH 12 or higher. The complexes $Co(CN)_5I^{3-}$ and $Co(CN)_5Br^{3-}$ give rise to the largest adsorption peaks and show very

FIG. 2. Adsorption peak currents vs. exposure potentials.

All solutions contained 1 mM complex and 1 F $NaClO_4$.

Scan rate = 10 V/sec.

Electrode area = 0.032 cm^2.

1 -- $Co(CN)_5I^{3-}$, pH 9

2 -- $Co(CN)_5^{3-}$, pH 10

3 -- $Co(CN)_5Br^{3-}$, pH 9

4 -- $Co(CN)_5H_2O^{2-}$, pH 4.1

5 -- $Co(CN)_5Cl^{3-}$, pH 4.5

6 -- $Co(CN)_5N_3^{3-}$, pH 4.7

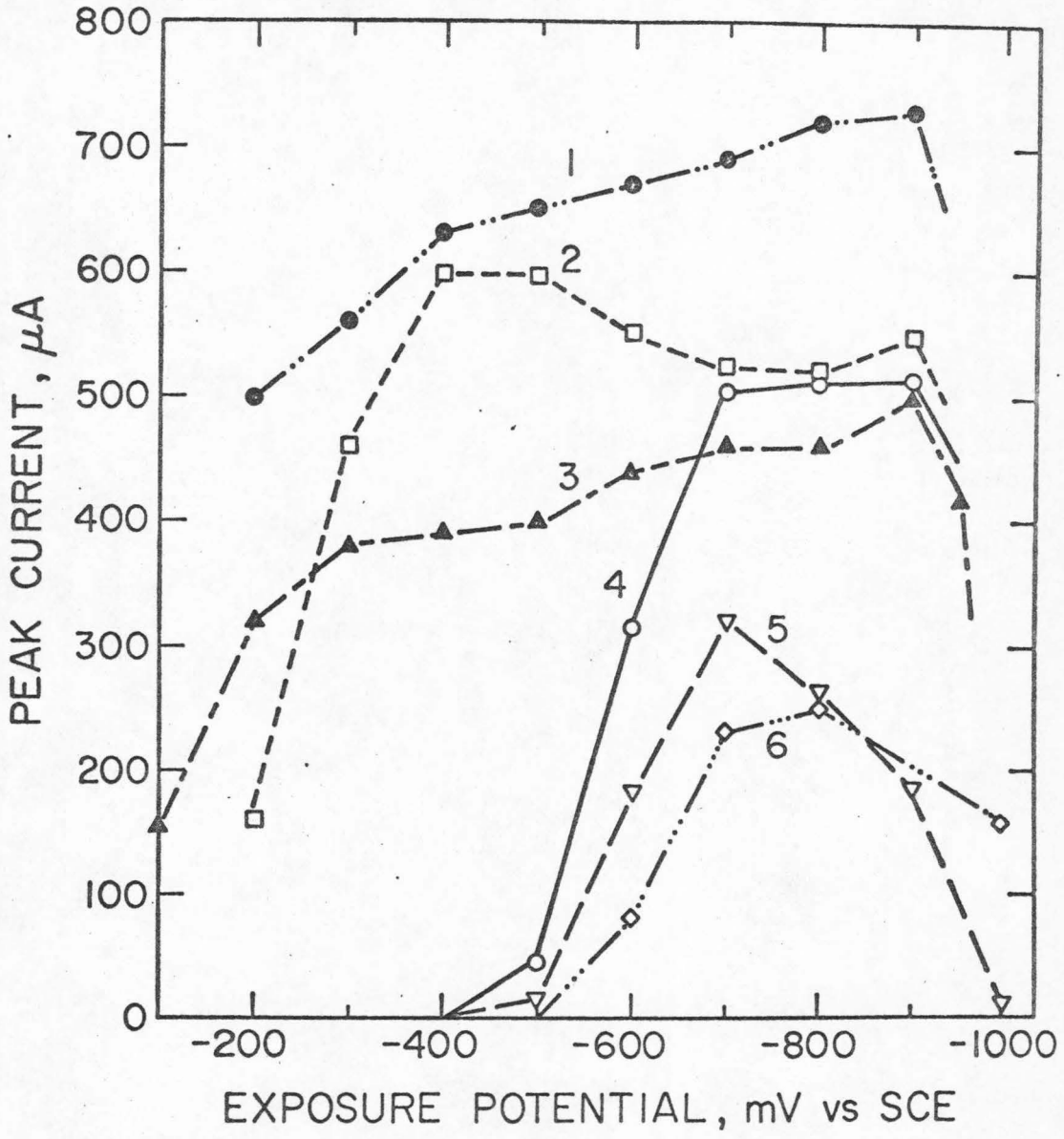
800
700
600
500
400
300
200
100
0
PEAK CURRENT, μA
-200
-400
-600
-800
-1000
EXPOSURE POTENTIAL, mV vs SCE
1
2
3
4
5
6

little pH dependence in the pH range 4-9. By contrast, complexes such as $Co(CN)_5H_2O^{2-}$, which produce smaller adsorption peak currents (Fig. 2), show a strong pH dependence at all pH values up to ca. pH 9 where the adsorption peak disappears.

Free cyanide ion strongly inhibits the adsorption peaks with all complexes, while chloride and bromide ion have no effect and iodide ion begins to cause a decrease in the adsorption only at concentrations exceeding 10^{-2} M. The ability of cyanide ion to inhibit the adsorption at concentrations (1 mM) where iodide ion, although the more strongly adsorbed, produces no effect on the adsorption peak strongly suggests that the inhibition by cyanide arises from a shift in a cyanide-dependent equilibrium in the solution rather than from a competition for adsorption sites on the electrode surface.

Behavior at the Dropping Mercury Electrode

The dependences of the adsorption peak currents upon exposure potential (Fig. 2) suggest that the cobalt(III) complexes are reduced to a cobalt(II) species in the process that leads to the adsorption. Evidence supporting the occurrence of this proposed reduction was obtained by recording conventional d. m. e. polarograms of solutions of the cobalt(III) complexes at high current sensitivity. Figure 3 compares the currents obtained with several complexes at potentials well ahead of the main reduction wave corresponding to the conversion of Co(III) to Co(II). Note that the $Co(CN)_5I^{3-}$ and $Co(CN)_5Br^{3-}$ complexes, which give prominent adsorption peaks in their cyclic

FIG. 3. Residual currents at the d. m. e. at potentials ahead of the first reduction wave

1 -- 4 m$\underline{M}$ $Co(CN)_5I^{3-}$

2 -- 10 m$\underline{M}$ $Co(CN)_5Br^{3-}$

3 -- 10 m$\underline{M}$ $Co(CN)_5H_2O^{2-}$

4 -- 10 m$\underline{M}$ $Co(CN)_5N_3^{3-}$

5 -- No complex present

6 -- 1 m$\underline{M}$ $Co(CN)_5^{3-}$

Currents plotted are those at maximum drop area; for some complexes these were not the maximum currents during drop life. DME characteristics at open circuit in 1 $\underline{F}$ NaCl: drop time = 4.85 sec; m = 0.954 mg/sec.

All solutions contained 1 $\underline{F}$ $NaClO_4$ buffered at pH 9 (borate) T = 25°C.

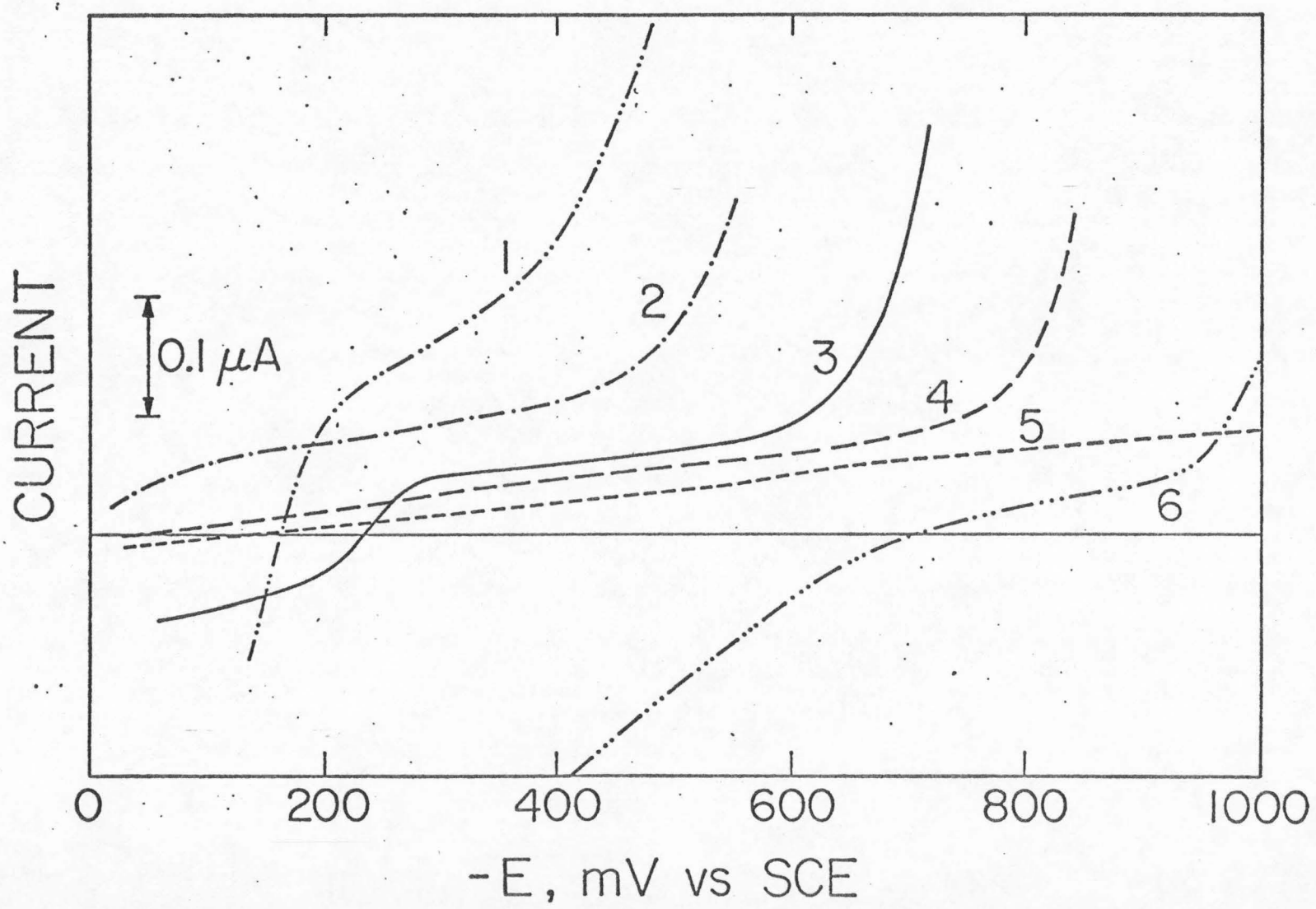
CURRENT
0.1 μA
1
2
3
4
5
6
0
200
400
600
800
1000
-E, mV vs SCE

voltammograms, produce much larger cathodic currents at potentials anodic of their main waves than do the $Co(CN)_5H_2O^{2-}$ and $Co(CN)_5N_3^{3-}$ complexes which show no adsorption peaks at pH 9. (The anodic currents obtained at potentials more positive than -200 mV appear to result from oxidation of the mercury electrode in the presence of certain of the cobalt(III) complexes. The exposure potentials were restricted to values more negative than -200 mV in our experiments to avoid this additional complication.) Although the magnitudes of these pre-currents are small, their existence is certain because the residual current obtained in the absence of any complex clearly increases upon addition of those complexes which give rise to an adsorption peak.

Residual currents in solutions of the labile cobalt(II) complex, $Co(CN)_5^{3-}$, are quite sensitive to the ratio of cobalt(II) to cyanide ion present, but net anodic currents are always observed at the d. m. e. at potentials more positive than ca. -700 mV. Between -700 and -800 mV very small residual currents are obtained although large adsorption peaks result in cyclic voltammetric experiments with exposure potentials of -700 or -800 mV. And at -900 mV a small cathodic residual current flows but the adsorption peak appears nevertheless. These differences between the residual currents in solutions of the cobalt(II) and cobalt(III) complexes which both produce the same adsorption peaks add support to the conclusion that the adsorbed species is a cobalt(II) complex.

Polarograms of both $Co(CN)_5X^{3-}$ and $Co(CN)_5^{3-}$ complexes display an indistinct but reproducible "pre-wave" at the foot of the wave corresponding to the reduction of cobalt(II) to cobalt(I) according to eqn. (2), as shown in Fig. 4. This wave is enhanced by decreasing the pH and depressed by the addition of free cyanide ion. Curve 1 in Fig. 4 shows a typical pre-wave observed at pH 10. Matschiner[2], who studied the behavior of this wave extensively, obtained considerably better separation of the pre-wave and main wave in the presence of gelatin added as a maximum suppressor. We confirmed this effect but preferred to work in gelatin-free solutions to avoid the possibility of any additional complication in an already exceedingly complex system.

Under conditions where the pre-wave was smaller than about one-half of the total wave, its magnitude was independent of the height of the mercury reservoir above the capillary. The main wave displayed the expected square-root dependence under the same conditions. This evidence for the kinetic character of the pre-wave agrees with that obtained by Matschiner[2] who concluded that the pre-wave arises from the reduction of $Co(CN)_4^{2-}$ formed at the

FIG. 4. Polarograms at the d. m. e. in 1 m$\underline{M}$ cobalt(II) solutions containing cyanide.

1. $[CN^-]/[Co(II)] = 4.9$
2. $[CN^-]/[Co(II)] = 6$

Solutions contained 0.05 $\underline{F}$ HCO_3^-–$CO_3^=$ buffer (pH = 10) and 0.95 $\underline{F}$ $NaClO_4$.

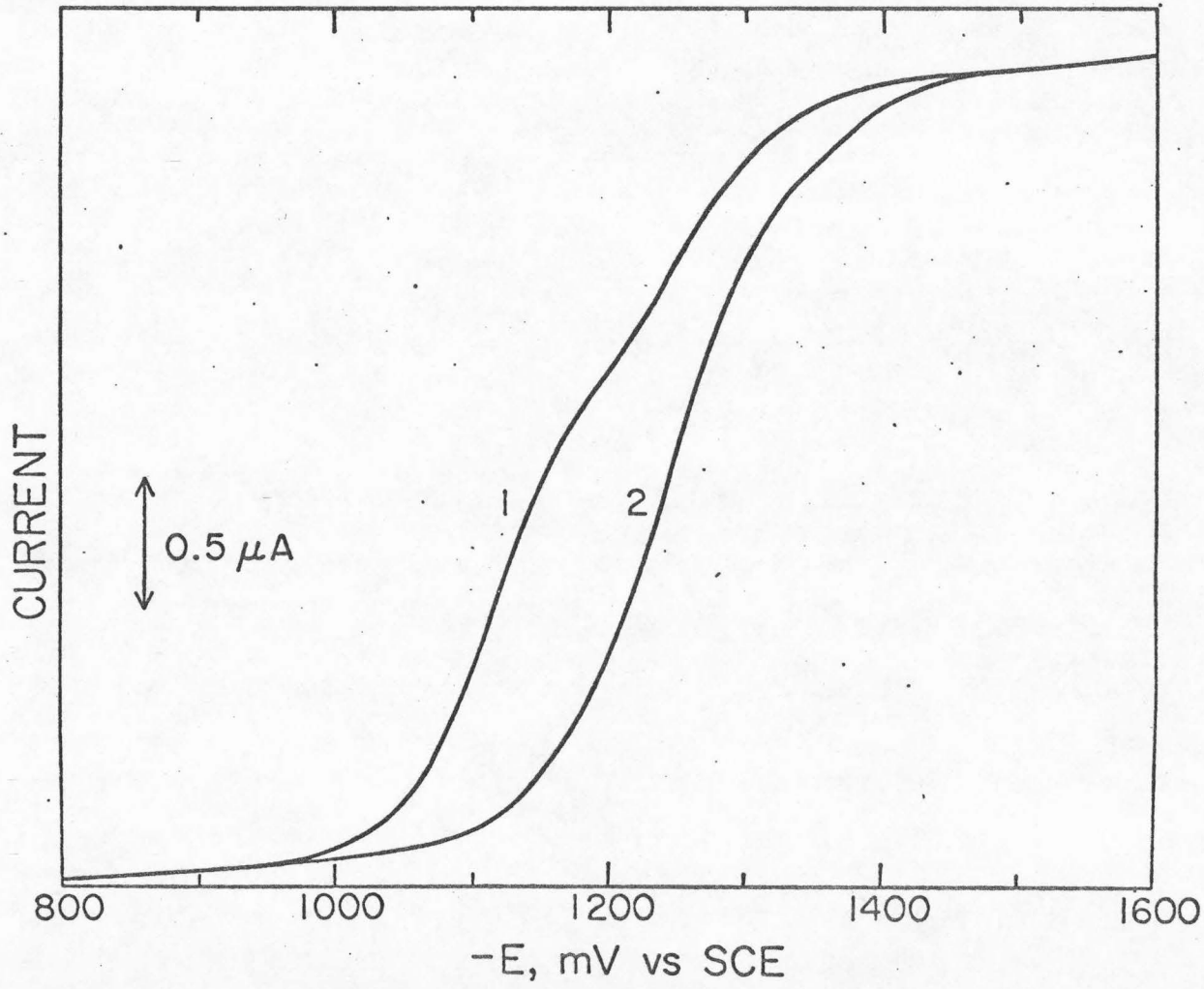
CURRENT
0.5 μA
1
2
800
1000
1200
1400
1600
-E, mV vs SCE

electrode surface accoding to reaction (4)

$$Co(CN)_5^{3-} = Co(CN)_4^{2-} + CN^- . \qquad (4)$$

The depression of the wave by cyanide ion is then attributed to the enhancement of the back reaction and the pH dependence is explained by the decrease in concentration of free cyanide ion at lower pH values. Of most relevance to the present study is the fact that this wave appears at a potential ($E_{1/2}$ = ca. -1100 mV at pH 10) close to that of the sharp adsorption peak in the linear potential scan experiments (E_p = ca. -1150). It is therefore appealing to propose that the adsorbed species may be the same complex, namely $Co(CN)_4^{2-}$, with the difference in potentials arising from stabilization of the complex by its adsorption. Additional evidence supporting this proposal will be described in a subsequent section.

Kinetic Effects of the Adsorbed Complex

The adsorption of an anionic species from solutions of $Co(CN)_5I^{3-}$ and $Co(CN)_5Br^{3-}$ would be expected to decrease the rates

of the irreversible reductions of these two complexes at the electrode because the potential, ϕ_2, at the Outer Helmholtz Plane[20] is made more negative by adsorption of anions. One result of this decrease in rate has already been noted in Fig. 1B: When adequate time is allowed for the adsorption to proceed to its maximum extent, the initial wave, I, corresponding to the reduction of cobalt(III) to cobalt(II), is virtually absent.

Figure 5 elaborates this effect in greater detail: The current-potential curves in the vicinity of the wave for the reduction of $Co(CN)_5I^{3-}$ to $Co(CN)_5^{3-}$ are shown as a function of the exposure time. The cathodic shift in the peak potential and the decreases in the peak currents at longer exposure times are the results of the increasing anion adsorption which leads to more negative values of ϕ_2 with a consequent decrease in the rate of reduction of the anionic complex, $Co(CN)_5I^{3-}$. The fact that this wave is virtually eliminated at longer exposure times means that the concentration of $Co(CN)_5X^{3-}$ at the electrode surface remains equal to its bulk concentration even at potentials just before those where the adsorption peak appears. Thus, a portion of the very large current that flows at this point results from a sudden increase in the rate of reduction of $Co(CN)_5X^{3-}$ as the anionic cobalt complex that suppresses the $Co(CN)_5X^{3-}$ reduction is itself reduced and desorbed.

Another example of the retardation of the cobalt(III) reduction rate is obtained from conventional d. m. e. polarographic measurements with solutions containing varying concentrations of the cobalt(III)

FIG. 5. Current-potential curves for $Co(CN)_5I^{3-}$ reduction after various exposure times.

Curve	Exposure time at -300 mV, sec	Adsorption peak current at -1150 mV, μA
1	2-3	85
2	10	210
3	30	370
4	50	500
5	70	590
6	50(stirred) + 20(unstirred)	610

Solution contained 1 m$\underline{M}$ $Co(CN)_5I^{3-}$ at pH 8 in unbuffered 1 $\underline{F}$ $NaClO_4$. Dotted line is background current when complex is absent.

Scan rate = 10 V/sec; electrode area = 0.032 cm^2.

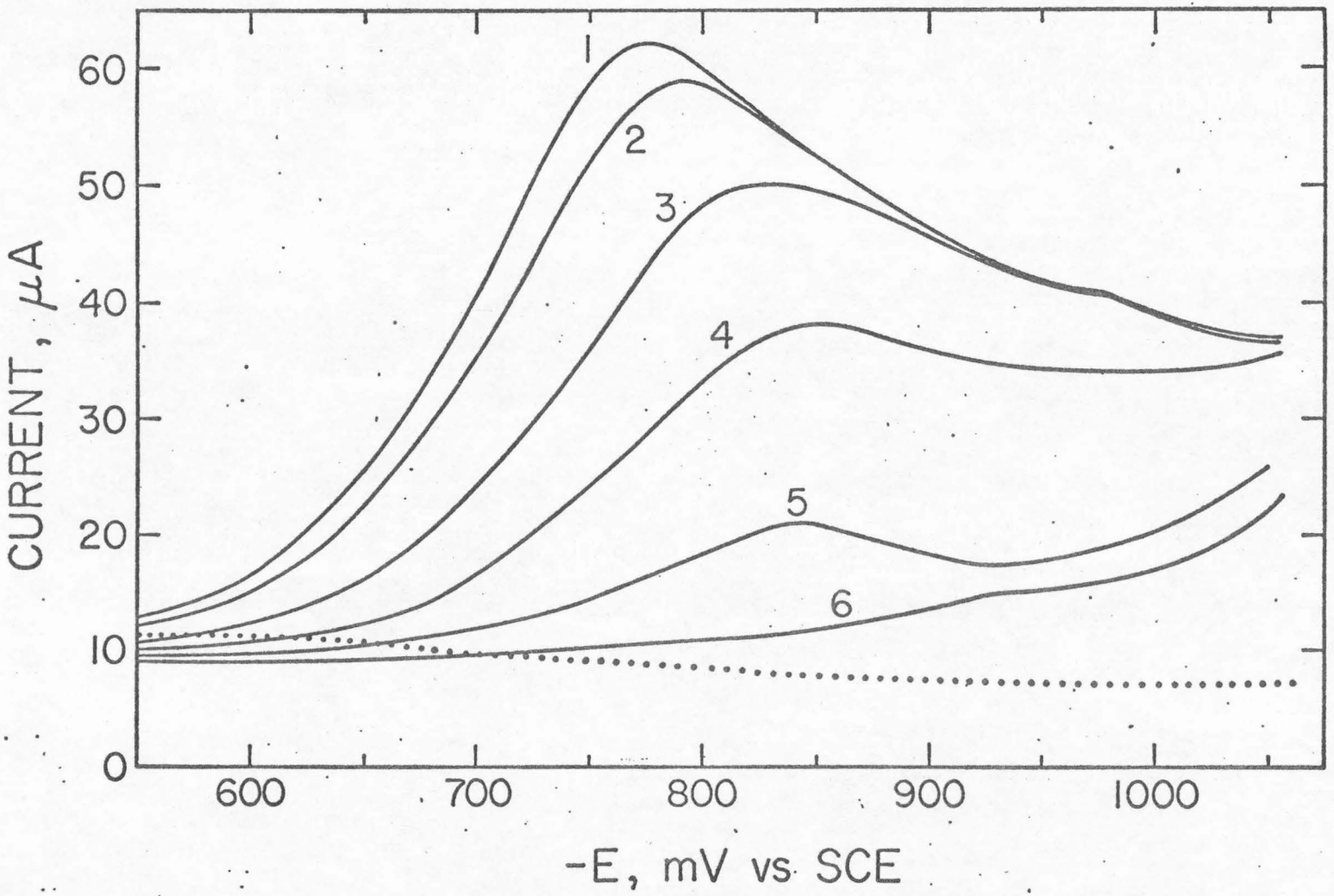
CURRENT, μA
0
10
20
30
40
50
60
600
700
800
900
1000
-E, mV vs SCE
1
2
3
4
5
6

complexes. Table 1 shows how the polarographic half-wave potential for the first wave [$Co(CN)_5X^{3-} + e^- \rightarrow Co(CN)_5^{3-} + X^-$] depends upon the concentration of the cobalt(III) complex. The shift of the $E_{1/2}$ values to more negative potentials as the concentration of the complex increases reflects the decrease in the rate of the electrode reaction produced by the increase in the quantity of the anionic complex adsorbed during drop life as the concentration of $Co(CN)_5X^{3-}$ increases *. The larger shifts in $E_{1/2}$ values at the lower ionic strength are to be expected because of the larger changes in ϕ_2 that result from the adsorption of anions at the lower ionic strength. The $E_{1/2}$ values for the last wave in the same polarograms [corresponding to $Co(CN)_5^{3-} + H_2O + e^- \rightarrow Co(CN)_5H^{3-} + OH^-$] remains at ca. -1250 mV at all concentrations of the complex because the adsorbed complex has been reduced and desorbed at potentials anodic of those where the last wave appears.

In solutions having pH values greater than 12, $Co(CN)_5I^{3-}$ does not give an adsorption peak in cyclic voltammetric experiments, even at exposure times greater than 100 seconds. However, in spite of this absence of an adsorption peak, the polarographic $E_{1/2}$ values for $Co(CN)_5I^{3-}$ at pH 12.5 continue to shift as the concentration of the

---

* The fact that a normal polarographic wave is obtained in solutions where linear potential scan gives almost no wave is a reflection of the much smaller amount of adsorption that is attained during the 4-5 second lifetime of a d.m.e..

TABLE 1

CONCENTRATION DEPENDENCE OF POLAROGRAPHIC HALF-WAVE POTENTIALS FOR

$Co(CN)_5X^{3-} + e^- \rightarrow Co(CN)_5^{3-} + X^-$ $(X = I^-, Br^-)$

$-E_{1/2}$, volts vs. S.C.E.

Complex Concentration, mM	$Co(CN)_5I^{3-}$			$Co(CN)_5Br^{3-}$	
	pH 9 $\mu = 0.1$	pH 9 $\mu = 1.0$	pH 12.5 $\mu = 1.0$	pH 9 $\mu = 1.0$	pH 12.5 $\mu = 1.0$
0.25	0.60	0.545	0.55	0.725	0.73
0.5	0.64	0.57	0.57	0.74	0.75
1.0	0.66	0.59	0.585	0.76	0.77
2.0	0.70	0.62	0.605	0.785	0.783
4.0	>0.75	>0.68			
10.0				0.82	0.81
0.5 + 0.75 mM $Co(CN)_5^{3-}$					0.775
0.5 + 0.05 mM Co^{2+}		>0.63			

complex is raised, and the shifts are in the same direction as is observed under conditions where the adsorption peak does appear. (See the entries in Table 1 for pH 12.5.) This behavior suggests that either $Co(CN)_5X^{3-}$ ($X = I^-$, Br^-) or $Co(CN)_5^{3-}$ (both are present at the electrode surface at $E_{1/2}$) are also adsorbed without giving rise to an adsorption peak. To examine this possibility the $E_{1/2}$ value for a solution containing 0.5 m$\underline{M}$ $Co(CN)_5Br^{3-}$ plus 0.75 m$\underline{M}$ $Co(CN)_5^{3-}$ at pH 12.5 was compared with the $E_{1/2}$ of a pure 2 m$\underline{M}$ $Co(CN)_5Br^{3-}$ solution. In both cases the electrode is exposed at $E_{1/2}$ to 1.0 m$\underline{M}$ $Co(CN)_5^{3-}$, but in the first case the electrode surface concentration of $Co(CN)_5Br^{3-}$ is 0.25 m$\underline{M}$ while in the second case it is 1.0 m$\underline{M}$. The result, included in Table 1, was that both solutions gave very nearly the same value of $E_{1/2}$ which was shifted cathodically from the $E_{1/2}$ of a pure 0.5 m$\underline{M}$ $Co(CN)_5Br^{3-}$ solution. The indication is, therefore, that adsorption of $Co(CN)_5^{3-}$ rather than $Co(CN)_5X^{3-}$ is primarily responsible for the cathodic shifts in $E_{1/2}$ potentials as the bulk concentration of $Co(CN)_5X^{3-}$ is increased at pH 12.5.

The adsorption of $Co(CN)_5^{3-}$ at the lower pH values, where the adsorption peak does develop, could also be used to explain the shifts in $E_{1/2}$ values shown in Table 1 at pH 9. However, a different adsorbing species is evidently responsible for the adsorption peak and probably also for the kinetic effects shown in Table 1 at pH 9. This conclusion follows from the fact that the rate of reduction of CrO_4^{2-} anions at pH 9 (in the pre-wave region[21]) is greatly decreased by the addition of 0.5 m$\underline{M}$ $Co(CN)_5I^{3-}$ to the chromate solution.

This effect occurs even at potentials, e.g., -300 mV, where the $Co(CN)_5I^{3-}$ is not reduced to $Co(CN)_5^{3-}$ but where, in the absence of the cobalt complex, CrO_4^{2-} displays a well-formed reduction wave. By contrast, when 1 mM $Co(CN)_5H_2O^{2-}$, which gives no adsorption peak at pH 9, is added to the chromate solution no change in the rate of chromate reduction results.

Chronocoulometric Measurements of Adsorption

Although the magnitude of adsorption peak currents for waves as sharp as those in Fig. 1 provides a reasonable qualitative estimate of the amount of adsorbed reactant present, we hoped to obtain more accurate values of the quantities of adsorbed reactant from chronocoulometric experiments [17].

Adsorption of $Co(CN)_5I^{3-}$

Attempts were first made to measure the adsorption, if any, of $Co(CN)_5I^{3-}$ by stepping the potential from an initial value anodic of the Co(III) to Co(II) wave, to -1000 mV, where reaction (1) proceeds at a diffusion controlled rate (under polarographic conditions) but where the species responsible for the adsorption peak is not reduced. Two sets of chronocoulometric plots (charge vs. $(time)^{1/2}$) resulting from these experiments are shown in Fig. 6. Plots 1 and 2 were obtained at high pH values where no adsorption peaks appear in linear potential scan experiments with solutions of $Co(CN)_5I^{3-}$ or $Co(CN)_5Br^{3-}$. The two lines have intercepts on the charge axis which exceed the

FIG. 6. Chronocoulometric plots for reduction of $Co(CN)_5X^{3-}$ ($X^- = I^-$, Br^-) at -1000 mV.

1 -- 0.5 m<u>M</u> $Co(CN)_5I^{3-}$ in 1 <u>F</u> $NaClO_4$ at pH 12. Potential stepped from -300 to -1000 mV.

2 -- 0.5 m<u>M</u> $Co(CN)_5Br^{3-}$ in 1 <u>F</u> $NaClO_4$ at pH 12.5. Potential stepped from -200 to -1000 mV.

3 -- As in 1 except pH = 8.0.

The double layer charging blank, $Q_{d.\ell.}$, was subtracted before plotting the data.

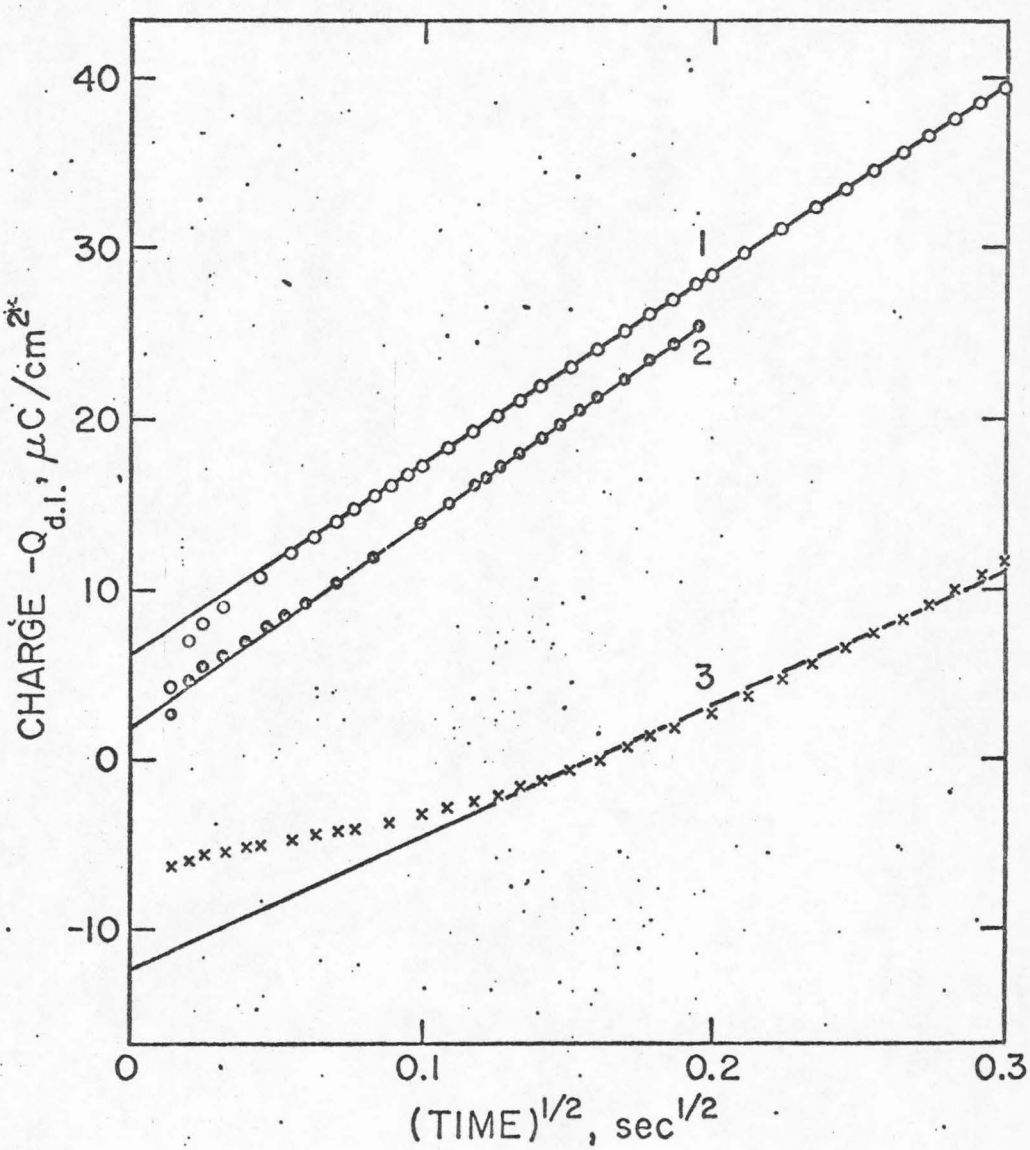
40
30
20
10
0
-10
0
0.1
0.2
0.3
1
2
3
CHARGE $-Q_{d.l.}$, $\mu C/cm^2$
$(TIME)^{1/2}$, $sec^{1/2}$

blank values, $Q_{d.\ell.}$, corresponding to the change in double layer charge, by ca. 7 $\mu C/cm^2$ with $Co(CN)_5I^{3-}$ and ca. 2 $\mu C/cm^2$ with $Co(CN)_5Br^{3-}$ indicating that both complexes are weakly adsorbed on the electrode, the iodo complex somewhat more extensively than the bromo complex.

The slopes of lines 1 and 2 in Fig. 6 correspond to reasonable values for the diffusion coefficients of the complexes ($D = 5 \times 10^{-6}$ cm^2/sec) and are the basis for some forthcoming comparisons of observed slopes with diffusion limited slopes.

Plot 3 in Fig. 6 resulted when the pH of the solution was lowered to 8.0 where a large adsorption peak is obtained in linear potential scan experiments. The slope of the line drawn through the later data points is only about half as large as those of lines 1 and 2 and its intercept on the charge axis becomes negative after the double layer blank is subtracted. The lower slope and intercept of line 3 are the chronocoulometric counterparts of the previously cited observation, Fig. 5, that the reduction current of $Co(CN)_5I^{3-}$ in linear potential scan experiments is reduced in magnitude as the adsorption of the cobalt complex increases. This inhibition of reaction (1) by the adsorbed species at pH 8 prevented the use of chronocoulometric experiments for determining whether any $Co(CN)_5I^{3-}$ is adsorbed when the adsorption peak is present. The fact that the data points fall below the double layer charging blank at times as long as 10 msec indicates that the integral double layer capacitance is lowered by the adsorption of the species which gives rise to the adsorption peak.

Adsorption of $Co(CN)_5^{3-}$

The polarographic data in Table 1 gave evidence of significant adsorption of the cobalt(II) complex, $Co(CN)_5^{3-}$. Verification of this adsorption by means of chronocoulometric measurements with solutions of $Co(CN)_5^{3-}$ was attempted by stepping the electrode potential from initial values where the complex was stable to -1500 mV, where it is reduced to cobalt(I) at a diffusion limited rate. The intercepts of the resulting chronocoulometric plots, corrected for the double layer charge by repeating the experiments without the complex, produced the values of adsorbed $Co(CN)_5^{3-}$ plotted as a function of the initial potential in Fig. 7, curve 1. With the conditions employed in these experiments, i.e., excess cyanide ion present, no adsorption peak appears in the cyclic voltammograms and the amount of adsorption found is independent of the exposure time. This behavior, as well as the decrease in adsorption at more negative potentials, is typical of the adsorption of simple anions which proceeds without significant prior chemical transformation of the anion[22]. This behavior contrasts with that obtained with the same complex in the absence of excess cyanide, curve 2 in Fig. 7, where the adsorption peak is present and the chronocoulometric intercepts, which reach very large values with increasing exposure times, are essentially independent of the exposure potential between -600 and -900 mV. These differences are believed to reflect two different adsorption processes, one similar to that involved in simple anion adsorption, and the other involving chemical transformation of the complex

FIG. 7. Potential dependence of the adsorption of $Co(CN)_5^{3-}$.

1 -- 0.25 m<u>M</u> $Co(CN)_5^{3-}$ and 1.25 m<u>M</u> CN^- in 1 <u>F</u> $NaClO_4$. Potential stepped from the exposure potential to -1500 mV. Values of $nF\Gamma$ were obtained by subtracting the double layer blank, $Q_{d.\ell.}$, from the intercepts of chronocoulometric plots.

2 -- 0.25 m<u>M</u> $Co(CN)_5^{3-}$ at pH 9.0 in unbuffered 1 <u>F</u> $NaClO_4$. Otherwise as in 1. The right-hand ordinate scale applies.

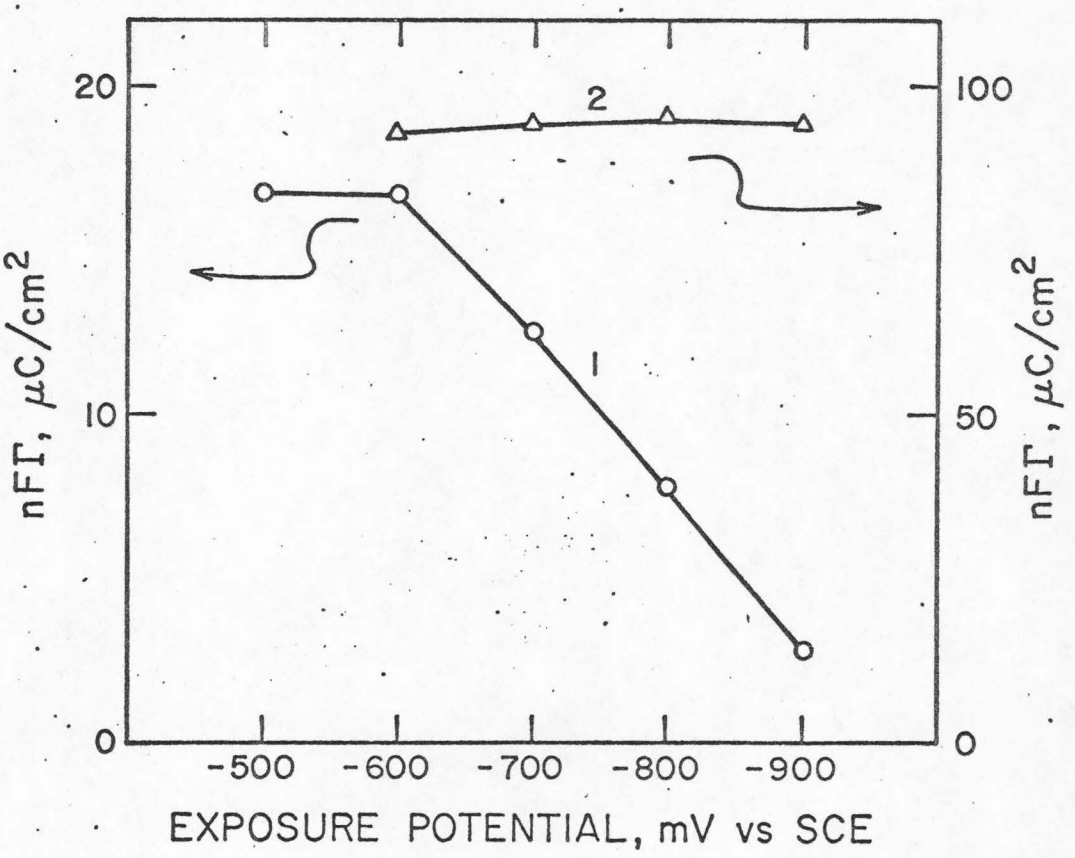
20
10
0
100
50
0
2
1
nFΓ, μC/cm²
nFΓ, μC/cm²
-500
-600
-700
-800
-900
EXPOSURE POTENTIAL, mV vs SCE

(e. g., by loss of a cyanide ion) as part of the adsorption process. A different mode of bonding between the electrode surface and the adsorbed species may be involved in the second process, e. g., a mercury-cobalt bond may be formed.

Adsorption of the Complex Responsible for the Peak

Chronocoulometric investigation of the species responsible for the adsorption peaks was attempted by stepping the potential from various initial values to a final potential, -1500 mV, well beyond the adsorption peak, where the reduction of all complexes to cobalt(I) was diffusion controlled. For cases in which no adsorption peak is obtained in linear potential scan experiments, e. g., $Co(CN)_5I^{3-}$ at pH 12, $Co(CN)_5H_2O^{2-}$ at pH 9.5, or $Co(CN)_5^{3-}$ with excess CN^- present, fairly normal chronocoulometric plots were obtained with slopes corresponding approximately to diffusion limited reduction of the complex to cobalt(I) and intercepts corresponding to small amounts of adsorbed complex: Fig. 8, curves 1, 2, and 3. However, in cases where the adsorption peak was present, e. g., $Co(CN)_5I^{3-}$ at pH 8 or $Co(CN)_5^{3-}$ with no excess CN^- present, very unusual chronocoulometric plots were obtained. Typically the plots had slopes considerably higher than would correspond to diffusion limited reduction of the complex and intercepts so high that several monolayers of a one-electron adsorbed reactant would be needed to account for them. Curves 4 and 5 in Fig. 8 show plots which display these anomalous features. The large deviations of the early data points in curves

FIG. 8. Chronocoulometric plots for reduction of several complexes at -1500 mV.

1 -- 0.5 m$\underline{M}$ $Co(CN)_5^{3-}$ + 0.5 m$\underline{M}$ CN^- at pH 10 in 1 $\underline{F}$ $NaClO_4$. Exposure potential = -800 mV, temp = 22°C.

2 -- 0.5 m$\underline{M}$ $Co(CN)_5H_2O^{2-}$ at pH 9.5 in 1 $\underline{F}$ $NaClO_4$. Exposure potential = -400 mV, temp = 25°C.

3 -- 0.5 m$\underline{M}$ $Co(CN)_5I^{3-}$ at pH 12 in 1 $\underline{F}$ $NaClO_4$. Exposure potential = -300 mV, temp = 22°C.

4 -- As in 1 except no excess CN^- present.

5 -- As in 3 except pH = 8.

The double layer charging blank, $Q_{d.\,\ell.}$, was subtracted from each point before plotting so that a line passing through the origin would correspond to no reactant adsorption.

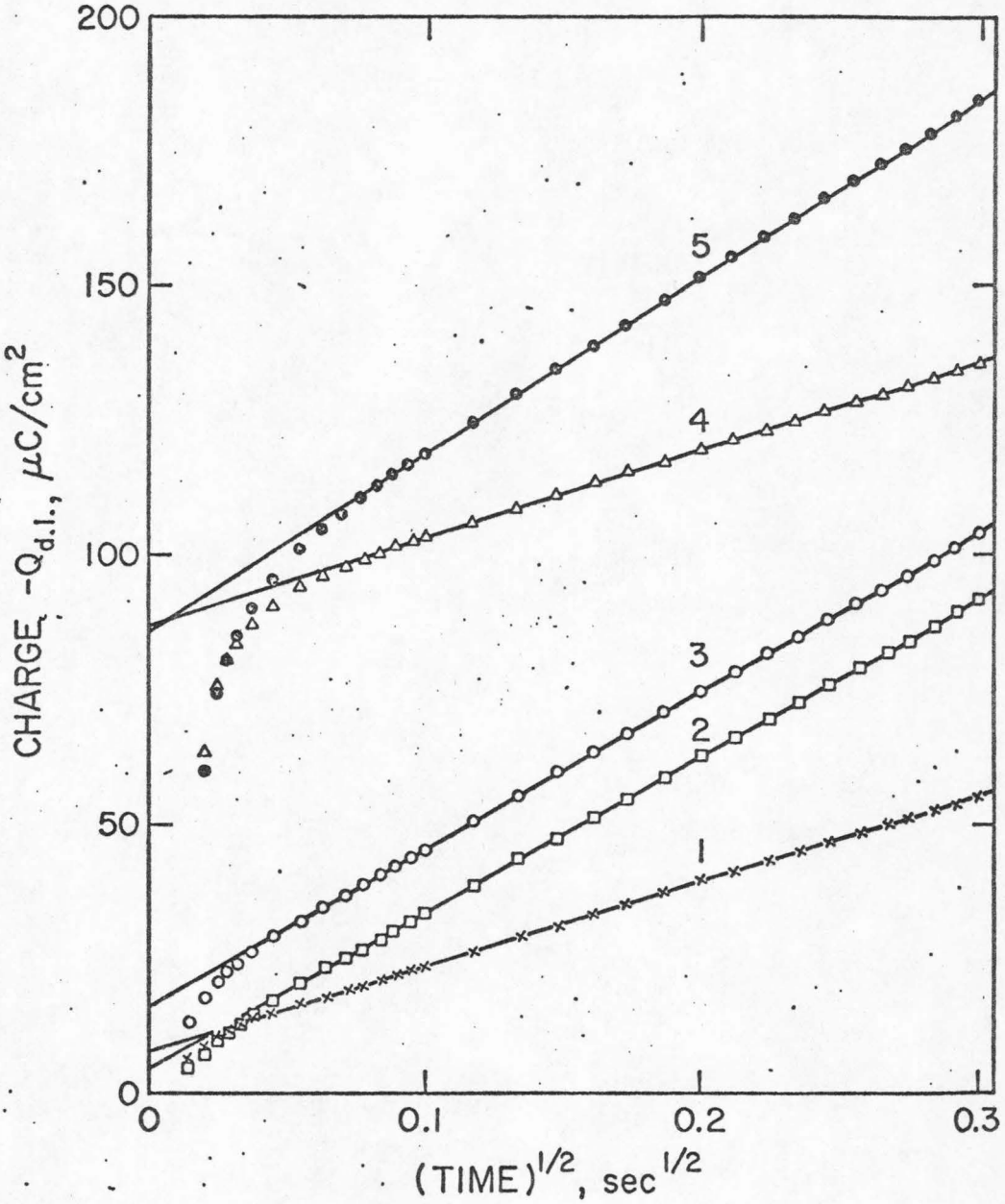
200
150
100
50
0
0
0.1
0.2
0.3
CHARGE, $-Q_{d.l.}$, $\mu C/cm^2$
$(TIME)^{1/2}$, $sec^{1/2}$
5
4
3
2
1

4 and 5 from the expected linear behavior obtained at longer times are the result of the small, unavoidable uncompensated resistance present in the cell[23]. The currents resulting from the reduction of the large quantities of adsorbed reactant reach such large values that residual uncompensated resistances, which are relatively innocuous in the absence of adsorbed reactant, produce delays approaching milliseconds in the arrival of the true electrode potential at -1500 mV. That the uncompensated resistance was responsible for the deviations was demonstrated by repeating the measurements using the technique of charge-step chronocoulometry[24] which allows observation of the rate of charge consumption at open circuit and is therefore immune to the difficulties introduced by the presence of uncompensated resistance. The resulting data points produced linear plots of charge vs. $(\text{time})^{1/2}$ with points falling on the straight line at times greater than 200 μsec.

The slopes of the charge-step and potential-step chronocoulometric plots are equal, as expected. However, the magnitude of the potential-step chronocoulometric slope is somewhat greater than twice the value corresponding to the diffusion limited reduction of the unadsorbed cobalt(III) complex to cobalt(II) (Fig. 6). This suggests that reduction of the adsorbed species leads to the continuous flow of some "extra" faradaic current even at times long after all of the adsorbed material has been reduced.

In spite of the difficulties produced by the presence of uncompensated resistances, the extrapolated intercepts of lines, such as

4 and 5 in Fig. 8 should provide reasonable estimates of the amounts of adsorbed complex. Indeed, these intercepts showed the same qualitative dependences upon the complex composition, initial exposure potential, time of exposure, and pH as did the adsorption peak currents obtained in the linear potential scan experiments, Fig. 2.

A revealing feature in the anomalous chronocoulometric plots obtained with $Co(CN)_5I^{3-}$ and $Co(CN)_5^{3-}$ is an approximately linear relation between their extrapolated intercepts and their slopes. Thus, if the initial exposure time of a new electrode to the solution is less than the 60 seconds normally employed, both the intercept and slope of the resulting charge-$(time)^{1/2}$ plot decrease. Data from a series of such experiments with varying exposure times are collected in Fig. 9. The fact that the smaller intercepts are accompanied by correspondingly smaller slopes strongly suggests that a species generated by the reduction of the adsorbed cobalt complex participates in whatever reaction cycle is responsible for the enhanced slopes of the chronocoulometric plots. Additional evidence supporting this possibility is the effect of temperature on the dependence of the slopes upon the intercepts of the chronocoulometric plots. As can be seen in Fig. 9, the dependence is essentially absent at 0°C and becomes more pronounced as the temperature is raised. This is the behavior to be expected from the thermal enhancement of the rates of additional reactions (chemical or electrochemical) that are initiated by the product of the reduction of the adsorbed cobalt complex.

FIG. 9. Relation between the apparent intercepts and slopes of chronocoulometric plots.

0.4 m$\underline{M}$ $Co(CN)_5I^{3-}$ at pH 8 in unbuffered 1 $\underline{F}$ $NaClO_4$. Exposure potential = -400 mV, potential stepped to -1500 mV.

1 -- 0°C.

2 -- 25°C.

3 -- 35°C.

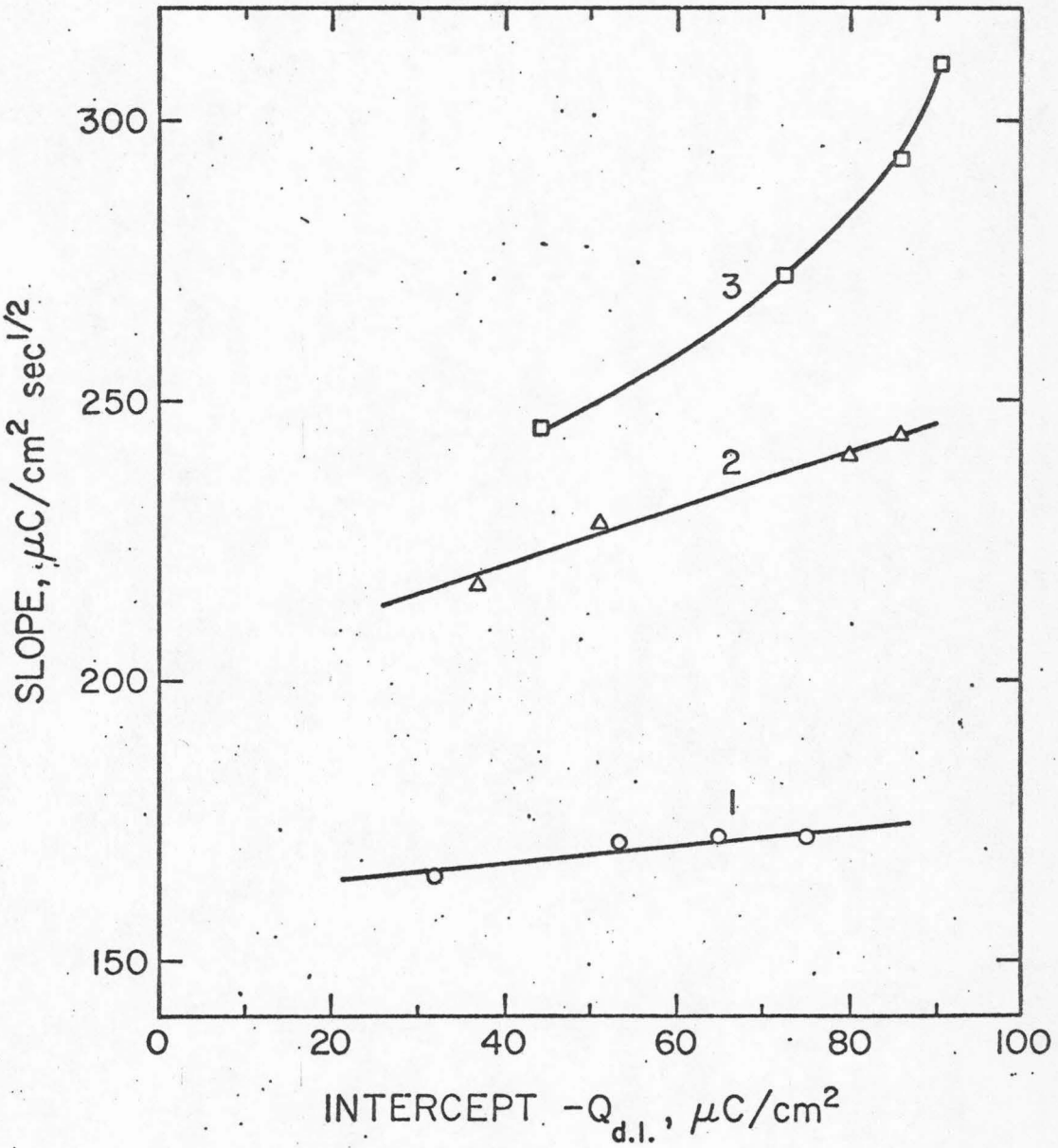
300
250
200
150
0
20
40
60
80
100
SLOPE, μC/cm² sec^1/2
INTERCEPT -Q_d.l., μC/cm²
1
2
3

Transient Anodic Wave Coupled to the Cathodic Adsorption Peak

Cyclic voltammograms of solutions of $Co(CN)_5X^{3-}$ or $Co(CN)_5^{3-}$ reveal no distinct anodic processes under most experimental conditions (Fig. 1) as would be expected from the highly irreversible nature of the electrode reactions involved. However, when the adsorption peak is present during an initial cathodic scan, a small wave appears during the subsequent anodic scan if the sweep rate is high enough. Figure 10 shows the anodic half of a set of cyclic voltammograms recorded after various exposure times. The anodic wave grows larger as the exposure times are lengthened producing larger adsorption peaks. It seems certain that this anodic wave is a counterpart of the cathodic adsorption peak because it appears only if the potential is allowed to traverse the region where the adsorption peak appears during the cathodic scan. The anodic wave does not appear if the solution is buffered so that the pH at the electrode surface is prevented from increasing (Fig. 10). The wave thus appears to represent an intermediate product of the electrode reaction which subsequently undergoes a pH-dependent conversion to a non-oxidizable form. The wave cannot correspond to the oxidation of $Co(CN)_5^{4-}$, which could conceivably be generated by the reduction of an adsorbed pentacyano cobaltate complex, because $Co(CN)_5^{4-}$ has been shown recently[25] to turn into the non-electroactive hydrido complex, via reaction (3), at a rate much too great for any of this complex to survive long enough to contribute to the anodic waves in Fig. 10. We believe the wave arises from a different hydrido complex

FIG. 10. Anodic wave coupled to the cathodic adsorption peak.

1.0 m<u>M</u> $Co(CN)_5I^{3-}$ at pH 8 in unbuffered 1 <u>F</u> $NaClO_4$.
Exposure potential = -300 mV; scan rate = 10 V/sec.
Exposure times and resulting adsorption peak currents at -1150 mV:

1 -- 2-3 sec, 85 μA

2 -- 10 sec, 210 μA

3 -- 50 sec, 500 μA

4 -- 50 sec(stirred) + 20 sec(unstirred), 610 μA

Dashed curve: background current in absence of complex.
Dotted curve: conditions as in curve 4 except solution buffered at pH 9 with borate.

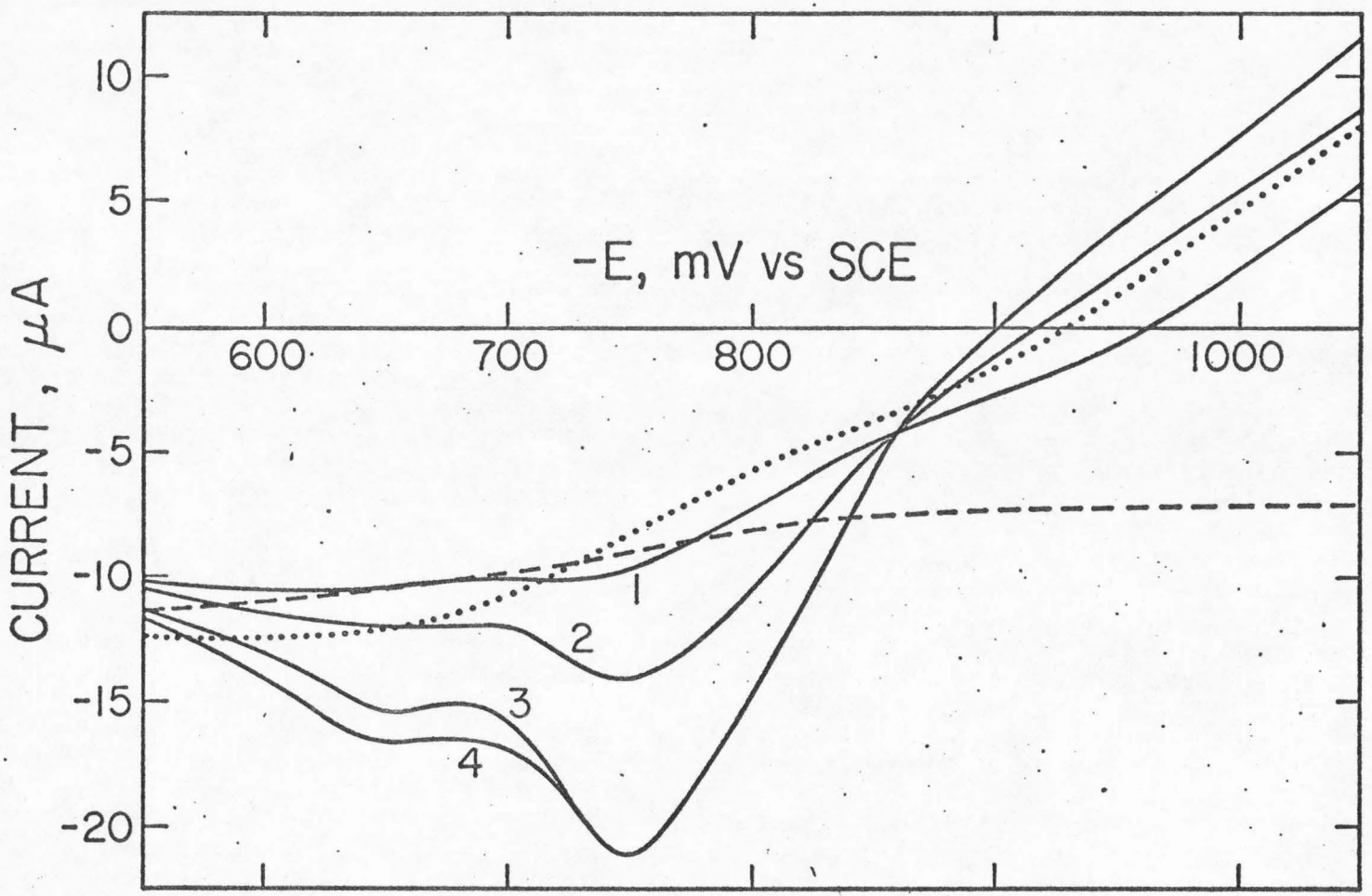
10
5
0
-5
-10
-15
-20
CURRENT, μA
-E, mV vs SCE
600
700
800
1000
1
2
3
4

containing fewer than five coordinated cyanide ions. The evidence for this assertion will be discussed in the subsequent section.

DISCUSSION

The unusual electrochemical behavior exhibited by pentacyanocobaltate complexes at mercury raises a number of questions. What is the formula of the species responsible for the adsorption peaks? What slow step is responsible for the time dependence of the adsorption peaks? What cycle of homogeneous and electrode reactions are involved in the additional faradaic process set off by the reduction of the adsorbed complex? We will offer possible answers to these and related questions on the basis of the results already described. It must be admitted at the outset, however, that the complexity of the behavior observed defies any relatively simple rationalizations (such as we will make) to account completely for all of its aspects.

Identity of the Adsorbed Complex

Modest adsorption of $Co(CN)_5X^{3-}$ ($X = I^-$, Br^-) and $Co(CN)_5^{3-}$, apparently without chemical transformation, has been shown to occur (Figs. 6 and 7) but these adsorbed reactants do not produce the unusually sharp adsorption peak. Considerable evidence can be cited to support the conclusion that the adsorbed species responsible for the adsorption peak is the same species regardless of the complex from which it is produced and that it is a cobalt(II) complex: The constancy of the potential at which the peak appears under widely varying

conditions attests to the uniqueness of the reducing species. The dependence of the peak currents and chronocoulometric intercepts upon the exposure potential, including the failure of the peak to appear at more positive exposure potentials in solutions of otherwise similar cobalt(III) complexes which are more difficult to reduce to cobalt(II) (Fig. 2), and the correlation between the occurrence of the peak and the flow of cathodic currents during the exposure time in cobalt(III) but not cobalt(II) solutions (Fig. 3), are two observations which support the contention that the adsorbed species contains cobalt(II).

The combination of available evidence points to $Co(CN)_4^{2-}$ as the adsorbed species with the fifth coordination position on the cobalt(II) probably utilized in bonding to the mercury surface. Three observations that support this proposal are the following: i) The potential at which the adsorption wave appears in cyclic voltammograms, -1150 mV, is within 50 mV of the $E_{1/2}$ of the polarographic pre-wave that has been attributed[2] to the reduction of unadsorbed $Co(CN)_4^{2-}$; ii) The adsorption peak (and the pre-wave) is inhibited by the presence of free cyanide ion. This fact cannot be explained if the species involved were $Co(CN)_5^{3-}$ because its adsorption is not inhibited by cyanide ion and there is almost no tendency for this complex to coordinate with another cyanide[26, 27]. On the other hand, it is readily accounted for if the rapid equilibrium reaction (5)

$$[Co(CN)_5^{3-}]_{ads} = [Co(CN)_4^{2-}]_{ads} + CN^- \qquad (5)$$

precedes the formation of the particular species which gives rise to

the adsorption peak. iii) The relative slowness of the adsorption process which leads to the development of adsorption peaks when compared with typical diffusion limited rates of simple anionic adsorption implies that bond breaking and making are involved in the adsorption process. There is no reason to expect a process such as $(NC)_4CoCN^{3-} + Hg \rightarrow (NC)_4CoCN^{3-}-Hg$ to proceed so slowly. By contrast, the alternative possibility:

$$[Co(CN)_4^{2-}]_{ads} + Hg \longrightarrow (NC)_4Co^{2-}-Hg \qquad (6)$$

might well proceed more slowly because of the low equilibrium concentration of $[Co(CN)_4^{2-}]_{ads}$ present and the necessity for forming the cobalt-mercury bond.

The adsorption process depicted in reaction (6) seems preferable to one in which linkage isomerism is invoked to account for the slow adsorption, e.g., reaction (7)

$$(NC)_4Co(CN)^{3-} + Hg \longrightarrow (NC)_4CoNC^{3-}-Hg \qquad (7)$$

because the linkage isomerization mechanism cannot account for the inhibition of the adsorption by free cyanide ion. In addition, the binding of the adsorbed complex to the electrode surface by a cobalt-mercury bond is attractive because of its similarity to the recently demonstrated homogeneous reaction between $Co(CN)_5^{4-}$ and Hg(II) to produce cobalt-mercury bonds [13] and because it provides a possible explanation for the observed potential dependence of the adsorption: The fact that the adsorption of an anionic complex increases

significantly as the electrode is made more negative (Fig. 2) requires a mode of bonding unlike that involved in the adsorption of simple anions on mercury which exhibits a potential dependence in the opposite direction[22]. This more familiar kind of anion adsorption is also observed in the case of $Co(CN)_5^{3-}$ in the presence of excess cyanide which displays the usual dependence of the adsorption on potential (Fig. 7). The decreasing adsorption at more negative potentials for these cases is generally attributed to the increasing coulombic repulsion between the electrode and the negative anions. On the other hand, it does not seem unreasonable that the adsorption of a coordinatively unsaturated complex by means of a cobalt-mercury bond could become stronger as the electrode is made more negative because the mercury surface can be regarded as a fifth ligand which uses its electrons to form the bond to the cobalt ion. The increase in bond strength with increasing electron availability (more negative charge on the electrode) could more than compensate for the simultaneous increase in coulombic repulsion between the electrode surface and the whole complex anion.

A reaction sequence leading from the cobalt(III) complex to the adsorbed cobalt(II) complex that is consistent with the observed behavior is the following:

$$Co(CN)_5X^{3-} + e^- \longrightarrow [Co(CN)_5^{3-}]_{ads} + X^- \qquad (8)$$

$$[Co(CN)_5^{3-}]_{ads} \overset{\text{fast}}{\rightleftharpoons} [Co(CN)_4^{2-}]_{ads} + CN^- \qquad (5)$$

$$[Co(CN)_4^{2-}]_{ads} + Hg \xrightarrow{\text{slow}} (CN)_4Co^{2-}\text{-}Hg \qquad (6)$$

The observation that reaction (8) apparently proceeds at potentials that are quite anodic of the main cobalt(III) reduction wave (Fig. 3) is interpretable by the assumption that the cobalt(II) product, $Co(CN)_5^{3-}$, is formed in the adsorbed state which could correspond to a significantly lower activation energy for reaction (8). The observed potential dependence of the adsorption results from the potential dependences of steps (8) and (6) combined with the potential dependence of the adsorption of $Co(CN)_5^{3-}$. The rate of reaction (8) and the extent of reaction (6) would both be expected to increase at more negative potentials while the adsorption of $Co(CN)_5^{3-}$ decreases (Fig. 7). The shape of the curves in Fig. 2 then reflects the dominance of reactions (8) and (6) at all but the most negative exposure potential (-1000 mV) where adsorption of $Co(CN)_5^{3-}$ is depressed and adsorbed $Co(CN)_4^{2-}$ may well be reductively desorbed.

The effects of changes in pH or cyanide ion concentration on the adsorption are both attributable to the shifts in equilibria (5) which they produce, i.e., any factor which decreases the cyanide concentration should enhance the adsorption, as is observed. Added evidence in support of this interpretation is the effect of additions of very small amounts of Co^{2+} ion to the solutions in which the adsorption processes are occurring. Co^{2+} ions act to shift equilibrium (5) to the right by combining with the cyanide ion released and, as expected, the rate of adsorption goes up. This is evident from the greater negative shifts in polarographic $E_{1/2}$ values in the presence of Co^{2+} (Table 1, final entry) and the fact that the residual currents obtained under the

conditions of Fig. 3 are significantly increased by the addition of Co^{2+}.

In strongly alkaline solutions of $Co(CN)_5H^{3-}$ an anodic polarographic wave appears which has been attributed to the oxidation of the $Co(CN)_5^{4-}$ formed by the reversal of reaction (3)[28]. The potential of this anodic wave, ca. -1050 mV, does not match the potential (ca. -750 mV) of the anodic wave that is obtained in cyclic voltammetry with solutions which show the adsorption peak (Fig. 10). Although some difference in potential would be expected because of the different observation techniques necessarily employed, the difference seems too large to be consistent with the same species' being responsible for both waves. This difference, as well as the previously cited evidence[25] that $Co(CN)_5^{4-}$ is too short-lived, requires that some other complex be responsible for the anodic wave.

Since the adsorbed complex must be anionic to account for its inhibiting action on the rate of reduction of the anionic cobalt(III) complexes (Fig. 5, Table 1), the two remaining possibilities for the adsorbed species are $Co(CN)_4^{2-}$ and $Co(CN)_3^{-}$. We prefer the former because, once the proposed Co–Hg bond is formed, no coordinative unsaturation remains.

Reaction Sequence Following Reduction of the Adsorbed Complex

A reaction sequence that leads to the consumption of several electrons for each molecule of adsorbed complex is needed to account for the unusually large adsorption peak currents and chronocoulometric intercepts obtained. The reaction sequence appears to be set off by

the short-lived complex, presumably $Co(CN)_4^{3-}$, produced by the reduction of the adsorbed $Co(CN)_4^{2-}$. A possible mechanism that includes these features is the following:

$$Hg\text{–}Co(CN)_4^{2-} + e^- \longrightarrow Hg\text{–}Co(CN)_4^{3-} \quad (9)$$

$$Hg\text{–}Co(CN)_4^{3-} + H_2O \longrightarrow HCo(CN)_4OH^{3-} + Hg \quad (10)$$

$$HCo(CN)_4OH^{3-} + 2\,e^- \longrightarrow HCo(CN)_4^{4-} + OH^- \quad (11)$$

$$HCo(CN)_4^{4-} + H_2O \rightleftharpoons H_2Co(CN)_4^{3-} + OH^- \quad (12)$$

$$H_2Co(CN)_4^{3-} \longrightarrow H_2\uparrow + Co(CN)_4^{3-}. \quad (13)$$

Reactions (9) and (11) are assumed to occur very rapidly at the peak potential and more cathodic potentials and reaction (10) is also assumed to proceed rapidly by analogy with the related reaction between unadsorbed $Co(CN)_5^{4-}$ and H_2O [25]. By the time reactions (9) through (11) have proceeded, three faradays of charge will have been consumed for each mole of $Co(CN)_4^{2-}$ initially present on the electrode and the large adsorption peak currents and chronocoulometric intercepts (Figs. 2 and 8) become (about three times) easier to rationalize. A monolayer of $Hg\text{–}Co(CN)_4^{2-}$ on the electrode surface would yield chronocoulometric intercepts of ca.

70 $\mu C/cm^2$ * if reactions (9) to (11) proceeded rapidly. Once all of the adsorbed cobalt(I) complex generated by reaction (9) is consumed (by reactions (10) and (11)), reaction (11) can no longer occur and the rate of charge consumption drops to the lower value determined by the rate at which the unadsorbed cobalt(III) complex can diffuse to the electrode. Thus, the abrupt fall in current once the adsorption peak has been passed in cyclic voltammetry (Fig. 1) turns out to be a natural consequence of the mechanism given by reactions (9)-(11). This is one of the more compelling features of this mechanism because alternative mechanisms which invoke a brief surge of catalyzed hydrogen evolution to explain the large currents have difficulties accounting for the sudden termination of the catalytic cycle.

Reactions (12) and (13) do not consume charge themselves but the $Co(CN)_4^{3-}$ complex that is a product of reaction (13) would enter the mechanism at reaction (10) and lead to additional charge consumption when reaction (11) reoccurred. The resulting catalytic cycle, leading to hydrogen evolution, can account for the slopes of the chronocoulometric plots at longer times exceeding the expected

---

* This value is obtained by assuming hexagonally close-packed spherical molecules of $Co(CN)_6^{3-}$ having a radius equal to the sum of the cobalt-carbon and carbon-nitrogen bond lengths (= 3.04 Å)[29] plus the van der Waals radius of nitrogen (1.5 Å). The value would not differ significantly if $Hg-Co(CN)_4^{2-}$ were assumed to be a square planar complex lying on the surface of the electrode.

diffusion limited values to a greater extent, the greater are the intercepts of the same plots (Fig. 9): The rate of reaction (13), which determines the "additional" contribution to the slopes, is greater, the larger the amount of the tetracyanocobaltate species generated by means of the adsorption.

Even in cases where the adsorption peak is not present, such as $Co(CN)_5H_2O^{2-}$ at pH 9.5 (Fig. 8, curve 2), the chronocoulometric curves give evidence of a small extra faradaic contribution to the charge in the form of slopes that are slightly higher than would correspond to simple diffusion limited, two-electron reduction of the complex (Fig. 6). In such cases it seems likely that the same reaction sequence is responsible for the extra current except that the essential tetracyano complex arises in a homogeneous step, viz:

$$Co(CN)_5H_2O^{2-} + 2\,e^- \longrightarrow Co(CN)_5^{4-} + H_2O \qquad (14)$$

$$Co(CN)_5^{4-} \begin{cases} + H_2O \longrightarrow HCo(CN)_5^{3-} + OH^- & (3) \\ - CN^- \rightleftharpoons Co(CN)_4^{3-} & (15) \end{cases}$$

$$Co(CN)_4^{3-} + H_2O \longrightarrow HCo(CN)_4OH^{3-} \qquad (16)$$

The product of reaction (16) then undergoes reaction (11) at the electrode yielding the additional current. The amount of extra current obtained depends upon the relative rates of reaction (3) and the combination of reactions (15) and (16). The chronocoulometric data indicate that about 90% of the $Co(CN)_5^{4-}$ is consumed by reaction (3) under the conditions prevailing for curve 2 in Fig. 8.

A second reaction sequence leading to catalyzed hydrogen evolution and involving the hydridopentacyanocobaltate(III) that is produced by reaction (3) can also be written:

$$Co(CN)_5^{3-} + e^- \xrightarrow{\text{fast}} Co(CN)_5^{4-} \qquad (2)$$

$$Co(CN)_5^{4-} + H_2O \xrightarrow{\text{fast}} HCo(CN)_5^{3-} + OH^- \qquad (3)$$

$$2\,HCo(CN)_5^{3-} \xrightarrow{k_{17}} 2\,Co(CN)_5^{3-} + H_2\,. \qquad (17)$$

However, this cycle of three reactions proceeds at a rate limited by reaction (17) whose second-order rate constant has been measured[30, 31] as $k_{17} = 4 \times 10^{-3}\ M^{-1}\ sec^{-1}$. This constant corresponds to a rate of $Co(CN)_5^{3-}$ production several orders of magnitude too low to account for the enhanced slopes obtained in the present experiments.

The anodic wave that appears whenever the adsorption peak is present (Fig. 10) could be due to the complex produced in reaction (11), $HCo(CN)_4^{4-}$. The polarography of the analogous carbonyl complex, $Co(CO)_4^-$, has been investigated by Vlček[32] who obtained a single anodic wave which was attributed to reaction (18)

$$2\,Co(CO)_4^- \xrightarrow{Hg} (CO)_4Co\text{–}Hg\text{–}Co(CO)_4 + 2\,e^-\,. \qquad (18)$$

The facts that the anodic wave obtained in the present study is absent from buffered solutions (Fig. 10) and is always much smaller than is expected if all of the product of the cathodic process were available

for reaction during the anodic cycle are readily explained if equilibrium in reaction (12) is assumed to lie far to the right at pH 8-9. The hexacoordinate bishydrido complex that results from this reaction would be expected to resemble $HCo(CN)_5^{3-}$ in not undergoing further reactions at the electrode. The magnitude of the anodic wave is then determined by how much of the $HCo(CN)_4^{4-}$ complex remains unconverted to $H_2Co(CN)_4^{3-}$ at the electrode surface in unbuffered solutions where the pH at the electrode surface can reach 11 to 12 as a result of reaction (11).

An alternative scheme which might be considered is one in which the most important role played by the adsorbed cobalt complex is to provide a site for hydrogen atom adsorption, thus stabilizing their formation sufficiently to lower the otherwise large hydrogen overvoltage on mercury. A catalyzed evolution of hydrogen would then ensue.

Although such a scheme could account for the large peak currents and chronocoulometric intercepts in terms of the extra charge consumed in the hydrogen evolution, it would suffer from the fact that no obvious terminating reaction to end the catalyzed hydrogen evolution suggests itself. In addition, the anodic wave is difficult to explain with such a scheme. For these reasons we prefer the mechanism involving reactions (9)-(13).

The mechanism given by reactions (9) to (11) represents a conventional ECE process[33], reactions (9), (10), and (11), with a pair of follow-up reactions, (12) and (13). An unconventional aspect

of the mechanism is the fact that the species responsible for the ECE cycle is generated slowly by means of a chemical reaction between the mercury electrode and a component of the solution. Another unusual feature is that the "C" of the "ECE" represents a chemical reaction between an adsorbed species and an unadsorbed species. It is thus a heterogeneous reaction whose rate could conceivably be affected by changes in electrode potential even though no net charge transfer is involved. The narrow range of potentials within which the adsorption peak rises and falls prevented this possibility from being tested.

Finally, although the cobalt-cyanide complexes studied here exhibited unanticipated complexity in their electrochemical behavior, the results obtained and the conclusions reached suggest a number of intriguing possibilities for continued investigation. The idea that catalytically active species can be generated spontaneously by reactions between the material of the electrode and appropriately chosen metal complexes is a relatively new prospect with considerable potential for exploitation. One such possibility would be an experimental test of the extent to which the unusual electrochemical behavior exhibited by the cyanide complexes of cobalt will also be encountered in the analogous carbonyl complexes.

REFERENCES

1. A. A. VLČEK, Pure Appl. Chem., 10 (1965) 61.
2. H. MATSCHINER, Thesis, Martin-Luther University, Halle-Wittenberg, 1963.
3. N. MAKI in Polarography 1964, Vol. 1, Macmillan & Co., Ltd., London, 1966, p. 505.
4. D. N. HUME AND I. M. KOLTHOFF, J. Amer. Chem. Soc., 71 (1949) 867.
5. R. GRASSI, A. HAIM AND W. K. WILMARTH, Inorg. Chem., 6 (1967) 237.
6. A. W. ADAMSON, J. Amer. Chem. Soc., 73 (1951) 5710.
7. A similar procedure to that employed for $K_3Co(CN)_5Cl$ (5) was used: $[Co(NH_3)_5I]I_2$ was reacted with KCN.
8. R. BARCA, J. ELLIS, M.-S. TSAO AND M. K. WILMARTH, Inorg. Chem., 6 (1967) 243.
9. J. L. BURMEISTER, Inorg. Chem., 3 (1964) 919.
10. G. G. SCHLESSINGER, Chem. Anal., 56 (1967) 48.
11. D. F. GUTTERMAN AND H. B. GRAY, J. Amer. Chem. Soc., 91 (1969) 3105.
12. J. J. ALEXANDER AND H. B. GRAY, J. Amer. Chem. Soc., 89 (1967) 3356.
13. H. S. LIM AND F. C. ANSON, Inorg. Chem., 10 (1971) 103.
14. G. LAUER, Ph. D. Thesis, California Institute of Technology, 1967.

15. F. C. ANSON AND P. PAYNE, J. Electroanal. Chem., 13 (1967) 35.

16. G. LAUER, R. ABEL AND F. C. ANSON, Anal. Chem., 39 (1967) 765.

17. F. C. ANSON, Anal. Chem., 38 (1966) 54.

18. J. H. CHRISTIE, R. A. OSTERYOUNG AND F. C. ANSON, J. Electroanal. Chem., 13 (1967) 236.

19. N. K. KING AND M. E. WINFIELD, J. Amer. Chem. Soc., 83 (1961) 3366.

20. P. DELAHAY, Double Layer and Electrode Kinetics, Interscience Publishers, New York, 1965, Ch. 9.

21. J. J. TONDEUR, A. DOMBRET AND L. GIERST, J. Electroanal. Chem., 3 (1962) 225.

22. Reference 20, Ch. 4.

23. G. LAUER AND R. A. OSTERYOUNG, Anal. Chem., 38 (1966) 1106.

24. F. C. ANSON, Anal. Chem., 38 (1966) 1924.

25. G. D. VENERABLE II, E. J. HART AND J. HALPERN, J. Amer. Chem. Soc., 91 (1969) 7538.

26. J. DANON, R. P. A. MUNIZ, A. O. CARIDE AND I. WOLFSON, J. Mol. Struct., 1 (1967-68) 127.

27. A. O. CARIDE, S. I. ZANETTE AND J. DANON, J. Chem. Phys., 52 (1970) 4911.

28. J. HANZLIK AND A. A. VLČEK, Chem. Commun., 47 (1969).

29. N. A. CURRY, Acta Crystallogr., 12 (1959) 674.

30. B. DeVRIES, J. Catal., 1 (1962) 489.

31. M. G. BURNETT, P. J. CONOLLY AND C. KEMBALL, J. Chem. Soc. (A), 800 (1967).

32. A. A. VLČEK, Coll. Czech. Chem. Commun., 24 (1959) 1748.

33. A. C. TESTA AND W. N. REINMUTH, Anal. Chem., 33 (1961) 1320.

Part III. Redox Potentials of Ruthenium Ammine Complexes and the Reduction of Pyrazine Coordinated to Ruthenium(II)

REDOX POTENTIALS OF RUTHENIUM AMMINE COMPLEXES AND THE REDUCTION OF COORDINATED PYRAZINE TO RUTHENIUM(II)

ABSTRACT

A number of formal redox potentials for $Ru^{III}(NH_3)_5L + e = Ru^{II}(NH_3)_5L$ and $Ru^{III}(NH_3)_4L_2 + e = Ru^{II}(NH_3)_4L_2$ (where L is various ligands) has been measured by cyclic voltammetry, potentiometry, and polarography. The resulting values are discussed in terms of the properties of the ligands, such as π-accepting capability. Reduction of coordinated pyrazine in the complexes, $Ru(NH_3)_5Pz^{2+}$, cis- and trans-$Ru(NH_3)_4Pz_2^{2+}$, on a mercury electrode has been observed. The behavior of this reduction at various pH values as well as the reoxidation of the reduction products are discussed.

INTRODUCTION

The solution chemistry of ruthenium amine complexes has received considerable attention[1] from a number of workers in recent years. The electrochemistry of these complexes, however, has been studied much less extensively. We report here on a number of aspects of the electrochemical behavior of ruthenium ammine complexes that we have been studying. One objective of the work was to compare the electrochemical reduction of pyrazine when it is coordinated to ruthenium(II) with its reduction when it is uncoordinated in order to

assess the importance of metal to ligand back-bonding on the reducibility of coordinated ligands.[2]

EXPERIMENTAL

Reagents

$[Ru(NH_3)_5Cl]Cl_2$ was prepared as described in the literature either from $[Ru(NH_3)_6]Cl_3$[3] (Matthey Bishop Inc.) or from $RuCl_3$[4] (Research Organic/Inorganic Chemical Corp.). $[Ru(NH_3)_5Br]Br_2$ was prepared similarly by treating $Ru(NH_3)_6Cl_3$ with refluxing HBr. Cis- and trans-$[Ru(NH_3)_4Cl_2]Cl$ were prepared as described by Gleu and Breuel.[5]

$[Ru(NH_3)_5NCS](ClO_4)_2$ was prepared as follows: A solution of $Ru(NH_3)_5Cl^{2+}$ ion was reduced at a mercury pool electrode to yield $Ru(NH_3)_5H_2O^{2+}$. Excess sodium thiocyanate was added and the resulting orange to red solution was reoxidized at the electrode to give a wine red solution from which solid $[Ru(NH_3)_5NCS](ClO_4)_2$ was isolated by addition of 5 F $NaClO_4$. The $Ru(NH_3)_5NCS^{2+}$ ion had adsorption maxima at 495 nm (ϵ = 3, 500) and 327 nm (ϵ = 520).

$[Ru(NH_3)_5Py](ClO_4)_2$ (where py = pyridine) was prepared as described by Ford et al.[6] $[Ru(NH_3)_5Pz](ClO_4)_2$[6] and cis- and trans-$[Ru(NH_3)_4Pz_2](ClO_4)_2$[7, 8] (where pz = pyrazine) were prepared as follows: One millimole of the corresponding chlorocomplex was converted to the trifluoroacetate salt by silver trifluoroacetate.[6] (The volume of the solution was 5-10 ml.) The pH of the solution

was adjusted to about 3 and then 1-1.5 gr of pyrazine was added. After the solution was deaerated by argon several pieces of amalgamated zinc were added and the solution was stirred in the dark for a time (pentaammine: ca. 0.5 hr, others: ca. 2 hr). The solution was filtered from the zinc amalgam and 8 F sodium perchlorate solution was added dropwise to precipitate the complex. After cooling the solid was collected by filtration and washed with ethanol and ether, and dried in a vacuum desiccator. Recrystallization: The crude complex was dissolved in a minimum volume of hot (60-70°) water (for the pentaammine complex) or hot 1 F pyrazine solution (for tetraammine complexes). The solution was filtered and cooled slowly with addition of a few drops of 8 F $NaClO_4$ solution. The recrystallized solid was washed with ethanol and ether and dried in a vacuum desiccator. The solid $[Ru(NH_3)_5Pz](ClO_4)_2$ gave spectra identical to that reported in reference 6 when it was dissolved in water. The bispyrazine complexes also gave spectral bands in the visible region matching those reported previously[7, 8] (cis-complex: λ_{max} = 398 and 472 nm, trans-complex: λ_{max} = 487 nm). However, all of these complexes were contaminated to some extent by purple complexes which appeared to be the pyrazine bridged diruthenium complexes. When aqueous solutions of the complexes were put onto a column of cation exchange resin (Biorad, AG 50W-X4, 100-200 mesh, sodium ion form) and eluted with 1 F NaCl solution a deep purple band was left behind after the elution of the complexes. This band was hardly elutable even with a saturated NaCl solution. The

contaminant in the mono-pyrazine complex was present in such small quantities that it did not appear to affect the electrochemical behavior. With the bis-pyrazine complexes, however, the contamination was more serious so that the electrochemical studies with these complexes were conducted with solutions that had been eluted from the cation exchange resin.

$[(NH_3)_5RuPzRu(NH_3)_5](C_7H_7SO_3)_4 \cdot 2H_2O$ [9] was prepared by reacting quantitative amounts of $[Ru(NH_3)_5Cl]Cl_2$ and pyrazine in a similar manner to that for the preparation of $[Ru(NH_3)_5Pz](ClO_4)_2$. The uv-visible spectra of the prepared complex were identical with the published. An ion exchange experiment with the diruthenium pyrazine complex indicated that it is not contaminated by $Ru(NH_3)_5Pz^{2+}$ ion. For electrochemical studies, the tosylate ion in the complex was replaced by chloride ion by an anion exchange (Amberlite IRA-400) column.

$Ru(NH_3)_5H_2O^{3+}$ ion was prepared in solution as follows: A solution of 2 m$\underline{M}$ $[Ru(NH_3)_5Cl]Cl_2$ in 0.2 $\underline{F}$ CF_3COONa was reduced at a mercury pool electrode at -0.7 V under argon atmosphere. The resulting solution was transferred by a platinum syringe to a solution containing enough silver trifluoroacetate to reoxidize the complex to ruthenium(III) and to precipitate chloride ion as AgCl. The solution was filtered from the precipitate and the excess Ag^+ ion was reduced to the metal at a mercury pool electrode at 0 V. The $Ru(NH_3)_5OH_2^{3+}$ was identified by its spectra. [10]

Cis- and trans-$Ru(NH_3)_4(H_2O)_2^{2+}$ ions were prepared by the reduction of the corresponding ruthenium(III) chlorocomplex to ruthenium(II) at a mercury pool electrode and the liberated chloride ion was not removed. Evidence by cyclic voltammetry showed that the complex formation between the ruthenium and chloride in this solution (millimolar concentration of Cl^- and ruthenium) was not important if the sweep rate is fast enough.

A stock solution of 8 F $NaClO_4$ was prepared from $HClO_4$ and Na_2CO_3 as described previously.[11]

Measurement of formal potentials

Potentiometric measurement -- A 2 millimolar solution of $Ru(NH_3)_5H_2O^{3+}$ in 0.2 F CF_3COONa was reduced at a mercury pool electrode until the concentrations of ruthenium(II) and ruthenium(III) were approximately the same. The exact concentrations of the complexes in each oxidation state were determined polarographically. The equilibrium potential of a hanging mercury drop electrode in the resulting solutions was read, by means of a digital pH meter. The process was repeated at various values of the solution pH. Formal potentials were calculated from these potential readings and the concentration data without attempting to correct for junction potentials.

Cyclic voltammetric measurements -- Cyclic voltamograms of the complexes which are substitution inert in both oxidation states were recorded on an X-Y recorder at a sweep rate of 50-400 mV/sec. Voltammograms of other complexes, such as $Ru(NH_3)_5Cl^{2+}$ which

rapidly aquates when it is reduced were recorded on a storage oscilloscope at a high sweep rate (10-26 V/sec).

Apparatus

The electronic apparatus employed for the cyclic voltammetry and conventional d. m. e. polarography has been described.[12] The electrodes used for cyclic voltammetry were either a commercially available Metrohm-type handing mercury drop electrode or a platinum ball attached to a fine platinum wire sealed in glass. The characteristics of the d. m. e. at open circuit in 1 F NaCl when h = 60 cm were: drop time = 4. 85 sec; m = 0. 954 mg/sec.

Potentials were measured with respect to a calomel electrode saturated with NaCl which had a potential 5-6 mV more negative than an S. C. E. and are reported as measured if not otherwise stated.

Spectra were recorded by a Cary Recording Spectrophotometer Model 11M.

RESULTS AND DISCUSSION

Formal potentials of some ruthenium(III/II)

Formal reduction potentials for a number of ruthenium ammine complexes were evaluated by cyclic voltammetry, potentiometry or standard d. m. e. polarography. In some cases the electrode reactions are followed by a fairly rapid further reaction of the initial electrode reaction product. In these cases conventional polarography

measurements cannot be used to estimate the formal potentials because the polarographic half-wave potentials become functions of the rate of the succeeding chemical reaction. An example of this situation is $Ru(NH_3)_5X^{2+}$ (X = Cl, Br and NCS) at the electrode where the initial Ru(II) complex produced undergoes hydrolysis at an appreciable rate:

$$Ru(NH_3)_5X^{2+} + e = Ru(NH_3)_5X^{+} \quad (1)$$

$$Ru(NH_3)_5X^{+} \xrightarrow{k} Ru(NH_3)_5H_2O^{2+} + X^{-} \quad (2)$$

In cases such as this the formal potential for the couple was evaluated from cyclic voltammetric curves recorded with potential sweep rates high enough to avoid the occurrence of the chemical reaction during the experiment.[13]

The value of the rate constant for reaction (2) when X = Cl is reported to be 4.7 sec^{-1} [14] which corresponds to a half-life for the $Ru(NH_3)_5Cl^{+}$ complex of 0.15 sec. The E^0 for reaction (1) could therefore be measured by sweeping a region of ca. 0.5 V at rates greater than ca. 10 V/sec provided the electrode reaction itself was fast enough. Fortunately, except for <u>trans</u>-$Ru(NH_3)_4Cl_2^{+}$ and <u>trans</u>-$Ru(NH_3)_4(H_2O)_2^{3+}$, all the complexes studied displayed reversible electrode reactions: The potential separations between cathodic and anodic peaks were close to the theoretical value, 58 mV, and peak potentials were independent of sweep rates. The two <u>trans</u>-tetra-ammine complexes gave peak potential separations significantly

greater than 58 mV and the individual peak potentials depended on the sweep rates. The values obtained for their formal potentials are therefore only approximations.

The values of the formal potentials evaluated in this study along with some values for related couples obtained by others are collected together in Table I. Fairly substantial differences exist between some previously reported potentials and those obtained in the present study (in the cases, $Ru(NH_3)_6^{3+/2+}$, $Ru(NH_3)_5OH_2^{3+/2+}$, $Ru(NH_3)_5Py^{3+/2+}$ and $(NH_3)_5RuPzRu(NH_3)_5^{5+/4+}$). Some portion of the discrepancies may be attributable to differences in ionic strengths and junction potentials but the differences in the cases of $Ru(NH_3)_5OH_2^{3+/2+}$ and $Ru(NH_3)_5Py^{3+/2+}$ seem too large to be accounted for in this way. We believe the present values are the more reliable. Overall, there is good qualitative agreement between the trends evident in the E^f values in Table I and the π-accepting ability of the ligands.

The formal potentials of Ru(III/II) complexes are expected to be sensitive to π-backbonding from metal to ligand because the electrons in the metal π orbitals are directly involved in the redox reaction. The π-backbonding tends to stabilize the overall metal π orbitals and would reduce electron repulsion energies in the metal. The stronger the π-backbonding the more the lower oxidation state, Ru(II), is stabilized relative to Ru(III). Thus, in the series of complexes $Ru(NH_3)_5L$, where L stands for a variety of ligands, more positive values of E^f are expected as the π-accepting capability of the ligand increases. Zwickel and Creutz [7] make the same point and

TABLE I

FORMAL POTENTIALS OF RUTHENIUM COMPLEXES

Redox couples	E^f, in mV vs normal hydrogen electrode	Supporting electrolytes
$Ru(NH_3)_5OH^{2+/1+}$	-420 [a, c]	0.2 - 1 F NaOH
$Ru(NH_3)_5Cl^{2+/1+}$	-42 [b]	0.2 F CF_3COONa or $NaClO_4$
$Ru(NH_3)_5Br^{2+/1+}$	-34 [b, k]	0.1 F $NaClO_4$
$Ru(NH_3)_6^{3+/2+}$	+51 [b], +100* [f]	0.1 F $NaBF_4$
$Ru(NH_3)_5H_2O^{3+/2+}$	+66 [a, b, c]; +160* [f]	0.1 F CF_3COONa and 0.1 F CF_3COOH
$Ru(NH_3)_5NCS^{2+/1+}$	+133 [b, k]	0.9 F NaF
$Ru(NH_3)_5Py^{3+/2+}$	+305 [b], +350* [g], +420* [h]	0.1 F CF_3COONa and 0.1 F CF_3COOH
$Ru(NH_3)_5N$-(C(=O)-NH_2)$^{3+/2+}$	+440* [h]	
$Ru(NH_3)_5N$-(C(=O)-OCH_3)$^{3+/2+}$	+460* [h]	
$Ru(NH_3)_5Pz^{3+/2+}$	+490 [b]	1 F NaCl
$Ru(NH_3)_5PzH^{4+/3+}$	(+685) [d]	

TABLE I (Cont'd)

$Ru(NH_3)_5N_2^{3+/2+}$	$(>950)^{j}$	
$cis\text{-}Ru(NH_3)_4Cl_2^{1+/o}$	-100^{b}	0.2 F CF_3COONa
$cis\text{-}Ru(NH_3)_4(H_2O)_2^{3+/2+}$	$+100^{b}$	0.2 F CF_3COONa
$cis\text{-}Ru(NH_3)_4(N\langle\bigcirc\rangle\text{-}C(=O)\text{-}NH_2)_2^{3+/2+}$	$+700^{*, h}$	
$cis\text{-}Ru(NH_3)_4(N\langle\bigcirc\rangle\text{-}C(=O)\text{-}OCH_3)_2^{3+/2+}$	$+740^{*, h}$	
$cis\text{-}Ru(NH_3)_4Pz_2^{3+/2+}$	$+860^{b}$	1 F NaCl
$trans\text{-}Ru(NH_3)_4Cl_2^{1+/o}$	$(-180)^{b, e}$	0.2 F CF_3COONa
$trans\text{-}Ru(NH_3)_4(H_2O)_2^{3+/2+}$	$(+20)^{b, e}$	0.2 F CF_3COONa
$trans\text{-}Ru(NH_3)_4Pz_2^{3+/2+}$	$+780^{b}$	1 F NaCl
$(NH_3)_5RuPzRu(NH_3)_5^{5+/4+}$	$+350^{b}$; $+400^{*, i}$	1 F NaCl (acidic pH's)
$(NH_3)_5RuPzRu(NH_3)_5^{6+/5+}$	$+740^{b}$; $+760^{*, i}$	1 F NaCl (acidic pH's)

* Values reported by others.

[a] By potentiometry.

TABLE I (Cont'd)

[b] By cyclic voltammetry. The values reported are the arithmetic average of the cathodic and anodic peak potentials. These will differ from the actual formal potentials by 30 log (D_{III}/D_{II}) mV, where D_{III} and D_{II} are the diffusion coefficients of the Ru(III) and Ru(II) complexes, respectively.

[c] By polarography.

[d] Calculated from pK_a values [6] for both oxidation states of the complex and the E^f value for the $Ru(NH_3)_5Pz^{3+/2+}$ couple.

[e] Approximate values at the sweep rate of 10 V/sec.

[f] T. J. Meyer and H. Taube, Inorg. Chem. 7, 2369 (1968).

[g] Reference 7.

[h] R. G. Gaunder and H. Taube, Inorg. Chem. 9, 2627 (1970).

[i] Reference 9.

[j] In 0.1 - 1 F $HClO_4$ by a graphite electrode. The minimum value was estimated from the oxidation peak potential by cyclic voltammetry assuming that the electron transfer is fast.

[k] Experiments done by D. J. Barclay.

have already reported a close relation between half-wave potentials and the degree of π-backbonding calculated from spectral data for the series $Ru(NH_3)_5L^{2+}$ where L is pyridine, isonicotinamide or methyl isonicotinate. The order of π-accepting tendency in the neutral ligands in Table I is $N_2 > Pz >$ isonicotinamide~methyl isonicotinate $>$ $Py > H_2O \sim NH_3$. The E^f values follow this same order, as expected.

In complexes containing non-π-accepting ligands the complexes which have negative ions as ligands show more negative E^f values than those having neutral ligands (Table I). This is a result in accord with standard interpretations [15] (NCS^- ion is considered to be a π-accepting ligand since it is bonded to ruthenium via its nitrogen end as will be discussed later.) Reasoning analogous to that used to rationalize the order of E^f values for complexes having π-accepting ligands can be applied to the complexes containing π-donor ligands (OH^-, Cl^- and Br^-). Here, the chief factor appears to be the repulsion between electrons in the metal and ligand π orbitals. The magnitude of this repulsion should be in the order of $OH^- > Cl^- > Br^- > I^-$ on the basis of the relative ionic sizes. The relative E^f values observed agree with this order. Kallen and Earley [16] have recently reported E^f values for $Ru(H_2O)_5L^{2+/1+}$ (where L = Cl, Br and I) which follow this same order.

The highly negative value of E^f of the pentammine hydroxo complex is probably due to the added effect of much stronger σ-bonding by OH^- than Cl^- or Br^-. For example, the formation constants of $FeCl^{2+}$ and $FeCl^+$ from Cl^- and Fe^{3+} and Fe^{2+}

respectively are not much different while the formation constant of $FeOH^{2+}$ is about 1000 times greater than that of $FeOH^{+}$.[17] These differences in the formation constants would correspond to a difference of 240 mV in E^f values for the two couples.

The effect on E^f of the substitution of a second ammonia by another ligand to give a cis-tetraammine complex appears to be a simple cumulative one. This is indicated qualitatively by the relative E^f values of the cis-complexes in Table I. A similar cumulative π-backdonation has also been reported in the cis-tetrammine ruthenium(II) complexes.[7] The situation in the case of the trans-complexes seems to be less clear.

The thiocyanate complex listed in Table I gives deep red-purple color in aqueous solution and is presumed to be the nitrogen-bonded isomer on the basis of the following evidence: Addition of Hg^{2+} ions to a solution of the complex produce an immediate change in color (the solution becomes almost colorless) which suggests the occurrence of reaction (3) as demonstrated by Armor and Haim in the case of Cr(III)-thiocyanate complexes.[18, 19]

$$Ru(NH_3)_5NCS^{2+} + Hg^{2+} \rightleftharpoons Ru(NH_3)_5NCSHg^{4+}. \qquad (3)$$

If excess bromide ion is added to the colorless solution the original spectra is restored as would be expected from the reversal of reaction (3) by the formation of $HgBr_2$. The fact that both $Ru(NH_3)_5NCS^{+}$ and $Ru(NH_3)_5NCS^{2+}$ spontaneously adsorb on the surface of mercury electrodes[19] is added evidence that the thiocyanate is

nitrogen-bonded: Both vanadium(III) and chromium(III) thiocyanate complexes display similar adsorption[20, 21] and they are known to be nitrogen-bonded complexes. (Thiocyanate is reported to be bonded by the nitrogen end in <u>trans</u>-$[Ru(NH_3)_4(CO)NCS]NCS$[22] although this does not make a good analogy to the pentaammine complex because in the carbonyl complex the bonding could be influenced by the carbonyl group which would influence the position <u>trans</u> to it.)

<u>Equilibrium constants</u>

It is possible to estimate some equilibrium constants of interest from the E^f values in Table I. The difference between the formal potentials in Table I for aquopentaammine and hydroxopentaammine complexes combined with the known pK_a (4.2) of $Ru(NH_3)_5H_2O^{3+}$[23] leads to a value of 12.3 for the pK_a of $Ru(NH_3)_5H_2O^{2+}$. A value of 10.7 has been reported for this constant[24] but the direct pH titration used to obtain this value must have suffered from the usual difficulties associated with titrating such a weak acid in aqueous media. The difference between the E^f values for the aquo and chloro pentammine couples combined with an average of the reported values of the equilibrium constant for reaction (4)[23, 24] (K_4 = 105 M^{-1})

$$Ru(NH_3)_5H_2O^{3+} + Cl^- = Ru(NH_3)_5Cl^{2+} + H_2O, \qquad (4)$$

leads to an estimated value of the equilibrium constant for reaction (5)

$$Ru(NH_3)_5H_2O^{2+} + Cl^- \underset{k_b}{\overset{k_f}{\rightleftharpoons}} Ru(NH_3)_5Cl^+ + H_2O \qquad (5)$$

$$K_5 = 1.6\ M^{-1}$$

The backward rate constant, k_b, for reaction (5) has been measured to be 4.7 sec^{-1}.[14] The resulting value of k_f (= $K_5 k_b$) is 7 M^{-1} sec^{-1} which is approximately 100 times larger than that of a similar reaction with a neutral ligand.[25]

Electrochemical Reduction of Pyrazine Coordinated to Ruthenium(II)

The reduction of the coordinated pyrazine can be observed at a mercury electrode in an aqueous solution containing the ruthenium(II) pyrazine complexes, $Ru(NH_3)_5Pz^{2+}$, cis-, and trans-$Ru(NH_3)_4Pz_2^{2+}$. $Ru(NH_3)_5Pz^{2+}$ gives a well-defined polarographic wave in neutral and alkaline solutions (Fig. 1). The current on the top of the wave depends linearly on the square root of mercury height indicating that it is a diffusion limited current. This diffusion current corresponds approximately to a two electron reduction when it is compared with those for reduction of other pentaammine ruthenium(III) complexes to ruthenium(II). As the solution becomes more acidic the wave appears as a kind of a shoulder of a huge wave which is probably due to a catalytized reduction of hydrogen ion. The half-wave potentials, as well as the cathodic peak potentials obtained by cyclic voltammetry at constant sweep rate, are linear functions of pH in the alkaline region (Fig. 2). The cyclic voltammetric peak potentials reach a limiting value (-1.43 ~ -1.45 V depending on sweep rate) in very alkaline solutions

FIG. 1. Polarograms of $Ru(NH_3)_5Pz^{2+}$ at 25° and $\mu = 1$ (0.9 F NaCl + buffer)

Conc. of the complex:

curves 1-4: 0.8 mM
curves 5-11: 1.0 mM

Buffers and pH

curves 1-4:	phosphate, pH = 4.82, 5.84, 6.87 and 7.69
curves 5-7:	borate, pH = 8.07, 9.02 and 10.13
curves 8-9:	phosphate, pH = 11.11 and 12.15
curve 10:	NaOH, pH = 13.1
curve 11:	1 F NaOH

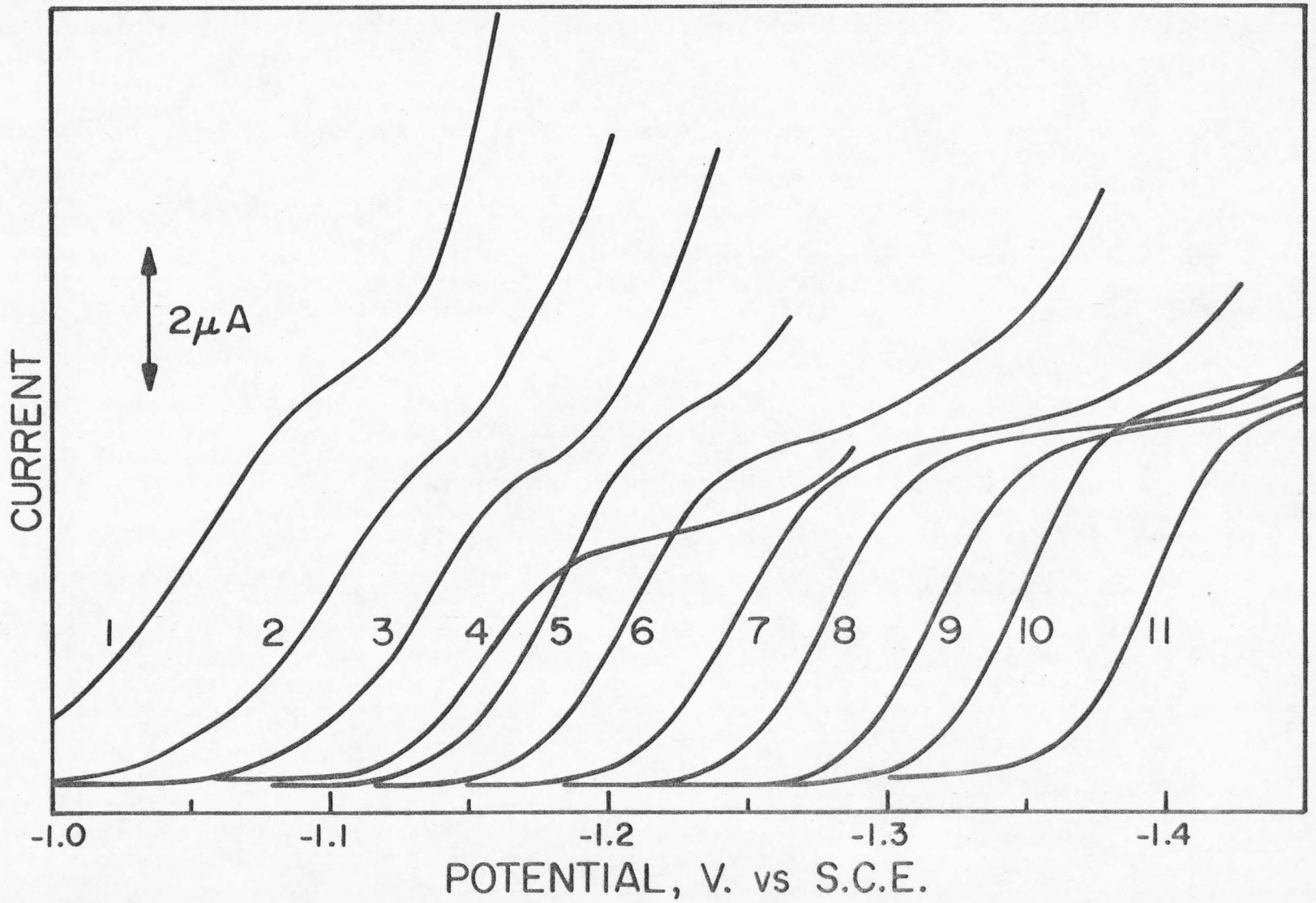
2μA
CURRENT
1
2
3
4
5
6
7
8
9
10
11
-1.0
-1.1
-1.2
-1.3
-1.4
POTENTIAL, V. vs S.C.E.

FIG. 2. Plots of polarographic half-wave potentials (□) and cathodic peak potentials (○) when sweep rate = 10 V/sec vs. pH.

Solutions: The same as in Fig. 1.

The pH values for pH ≥ 14 are based on the concentrations of NaOH.

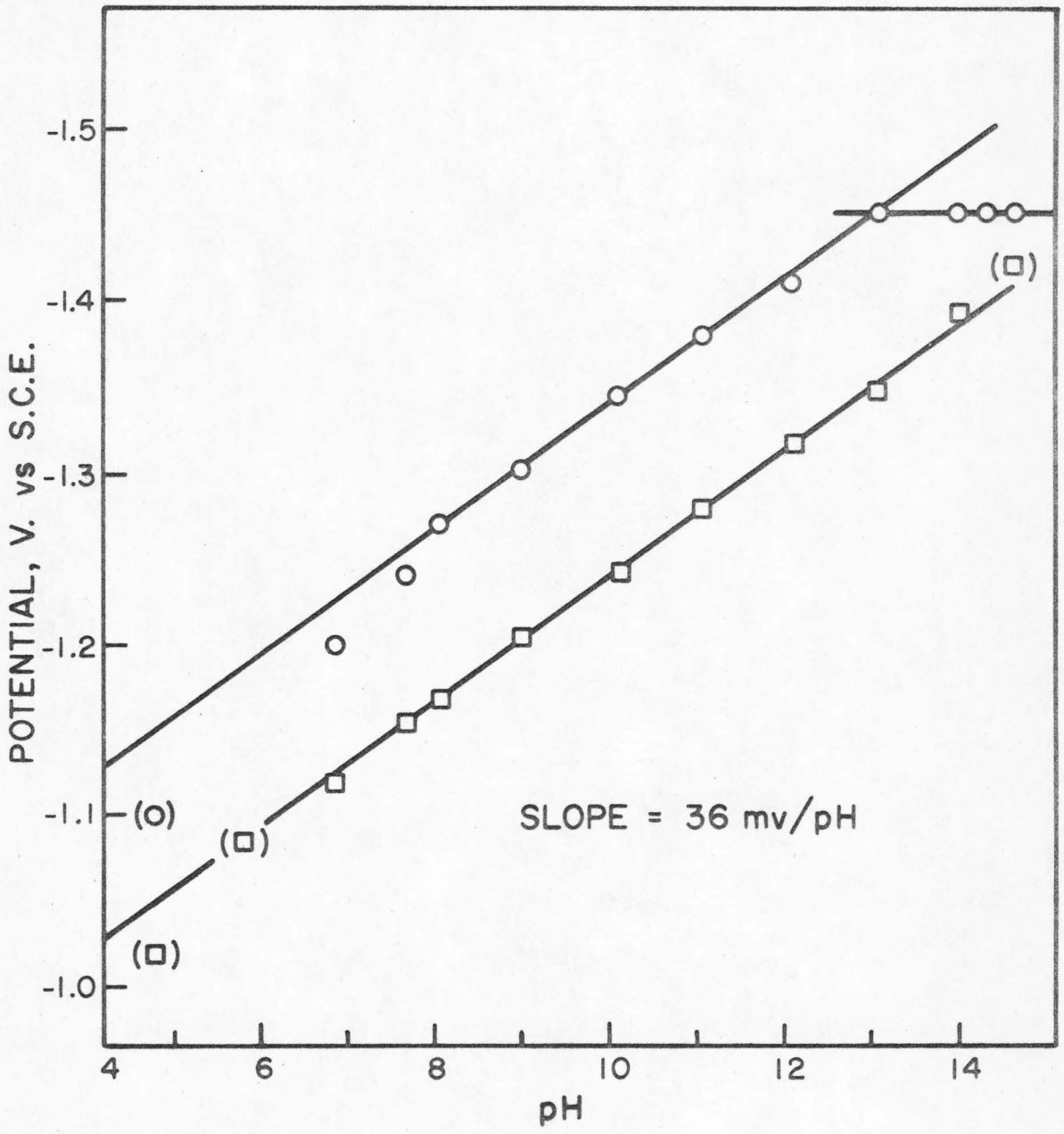
POTENTIAL, V. vs S.C.E.
-1.5
-1.4
-1.3
-1.2
-1.1
-1.0
(O)
(□)
(□)
(□)
SLOPE = 36 mv/pH
4
6
8
10
12
14
pH

(Fig. 2). These peak potentials become more cathodic with increasing sweep rates and the peak current displays a nonlinear dependence on the square root of sweep rate; increasing with sweep rate more rapidly than is expected for a simple diffusion limited charge-transfer reaction.[13]

A split of the cathodic wave (Fig. 3) is observed in acidic solutions of pH $<$ 5 but not in more alkaline solutions. This behavior may reflect the formation of a complexed radical, from the one-electron reduction of the coordinated pyrazine. Such radicals are known to be stabilized by protons when free pyrazine is reduced,[26, 27] but the available data are insufficient to prove that they can also be formed with coordinated pyrazine.

Typical cyclic voltammograms for the pyrazine complexes are shown in Fig. 3. Except in very acidic solutions a single anodic peak is coupled with the cathodic peak. The potential of the anodic peak stays at about -0.4 V at pH's from 3 to 9. If the pH is further increased this peak becomes broader and begins to shift cathodic and then the shape of the peak becomes normal again at very high pH's. In 4 F NaOH solution the cyclic voltammogram approaches that expected for a two-electron reversible couple. The cathodic and anodic peaks are separated by only 32 mV at a low-sweep rate (0.1 V/sec) and about 50 mV at 8 V/sec instead of 29 mV for a reversible couple.

FIG. 3. Cyclic voltammograms of $Ru(NH_3)_5Pz^{2+}$ at 25°.

1: pH = 4.8, phosphate buffer, v = 1.25 V/sec, μ = 1 (NaCl)

2: pH = 8.3, phosphate buffer, v = 10 V/sec, μ = 1 (NaCl)

3: pH = 12.5, phosphate buffer, v = 10 V/sec, μ = 1 (NaCl)

4: 1 F NaOH, v = 10 V/sec

5: 4 F NaOH, v = 8 V/sec.

Currents are in arbitrary scale.

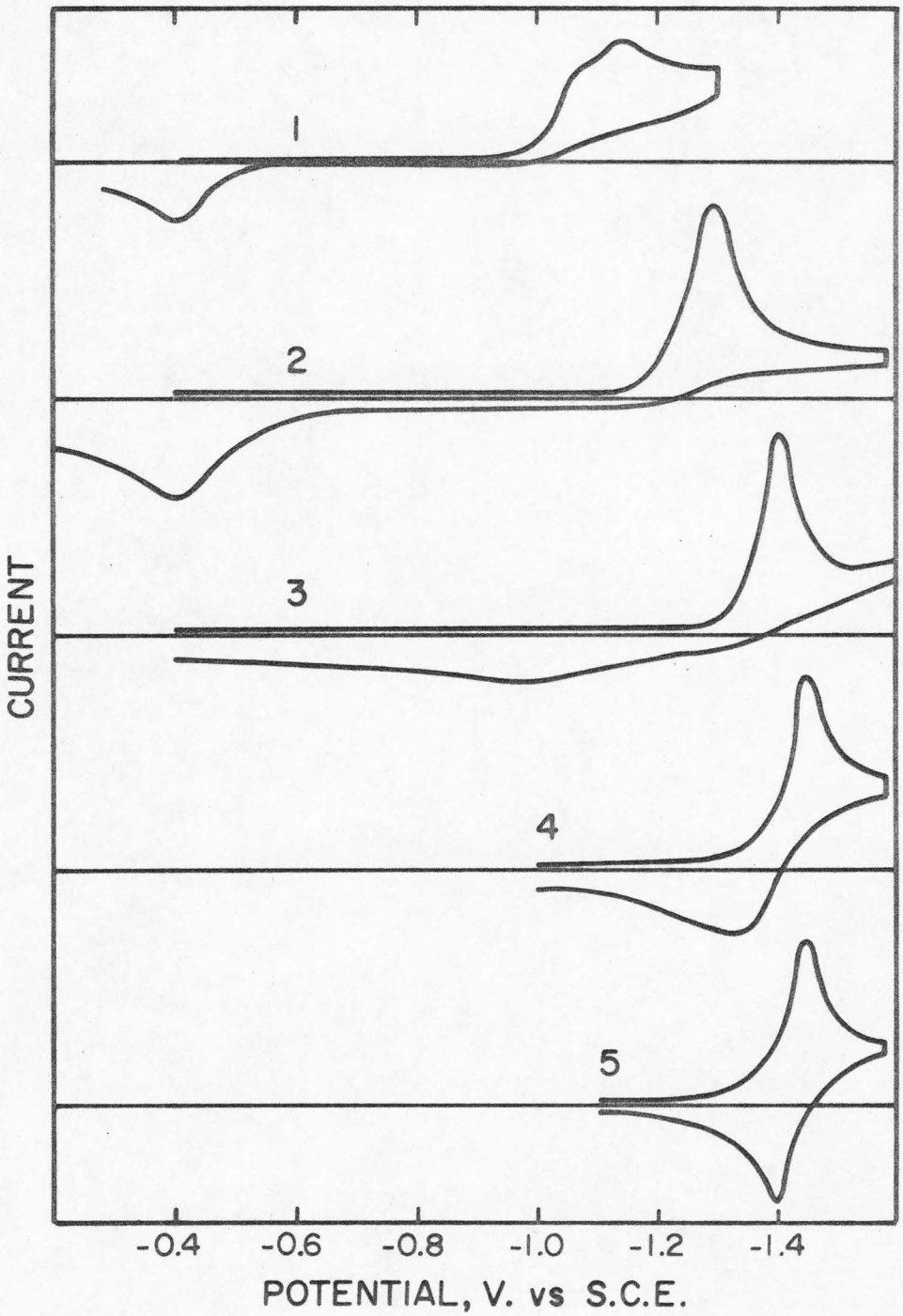
1
2
3
4
5
CURRENT
-0.4
-0.6
-0.8
-1.0
-1.2
-1.4
POTENTIAL, V. vs S.C.E.

On the basis of experimental results the following reactions appear to prevail in neutral and basic solutions:

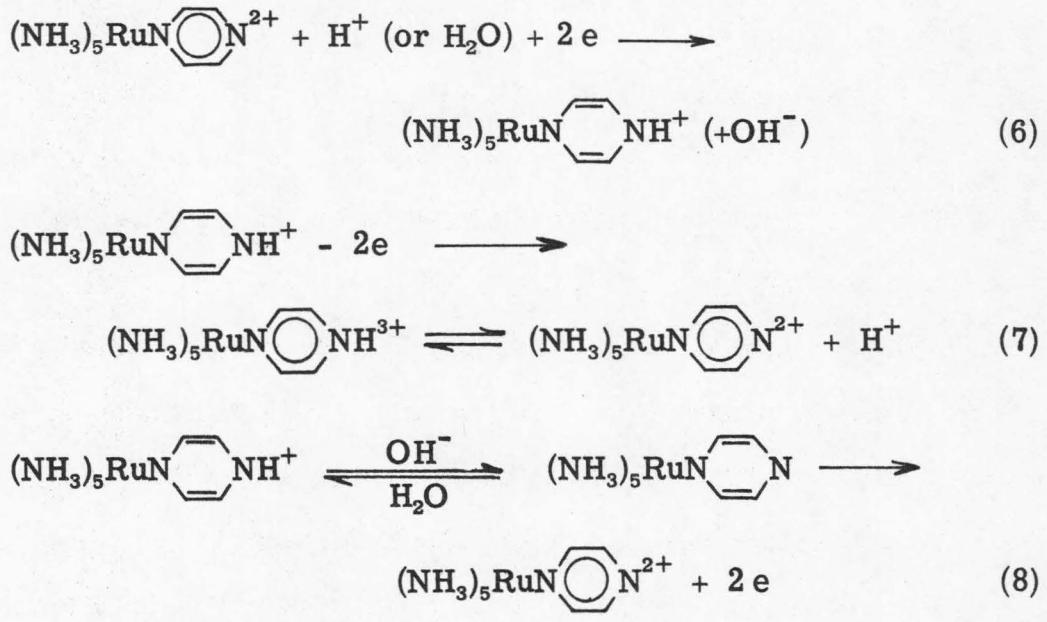

(6)

(7)

(8)

The detailed mechanism of reaction (6) can not be established unambiguously from the present experiments. Therefore the slope of Fig. 2 (36 mV/pH) may not be used to obtain reliable information about the number of hydrogen ions involved in the reduction of the complex. However, this number appears to be one for the following reason: As shown in Fig. 2, the cathodic peak potentials level off in highly alkaline solutions and so would the polarographic half-wave potentials because these potentials cannot be more negative than the peak potentials. This probably indicates that the pK_a value of $(NH_3)_5RuN$⟨⟩NH^+ for reaction,

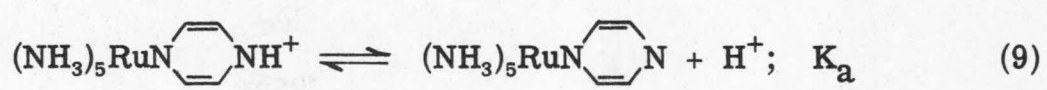

(9)

is around 15. This value of pK_a seems reasonable by comparison with those of organic amines of a similar kind (e.g., 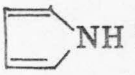 : pK_a = 15 - 16.5).[28] With this pK_a value reaction (9) would be shifted to the left except at very high pH values and the rate of reaction (8) would thus be limited by the rate of dissociation of the protonated complex. Therefore at low pH values, 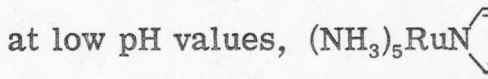 would be oxidized via reaction (7) and the oxidation potential would be independent of pH if the charge-transfer step is slow. Such an oxidation may be associated with the anodic peak at -0.4 V (Fig. 3) which is independent of pH in the pH range 5-9. The broad peaks at higher pH's can also be explained in terms of reaction (8) proceeding with a low but observable rate. With increasing pH this chemical reaction would become faster and finally the two reduced complexes in reaction (8) would be in a fast equilibrium. The observed voltammograms agree qualitatively with this explanation.

A more detailed study on the electrode reaction product, 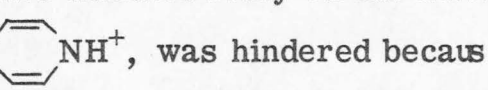 , was hindered because of the inherent instability of this complex in water. A complex containing a reduced pyrazine, 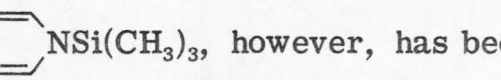 , however, has been isolated recently.[29]

<u>Cis</u>-$Ru(NH_3)_4Pz_2^{2+}$ ion gives a well-shaped polarographic wave at a potential slightly more anodic than that of $Ru(NH_3)_5Pz^{2+}$ and the wave height corresponds approximately to a four-electron reduction of the complex. The <u>trans</u>-complex begins to reduce at a more anodic potential than that of the <u>cis</u>-complex at a d. m. e. but a well-shaped wave is not obtained. The cyclic voltammograms of the bispyrazine

complexes are compared with that of the monopyrazine complex in Fig. 4. From the number of electrons (four) involved in the reduction of the bispyrazine complex, both pyrazines in the cis- and trans-complexes appear to be reduced to the same ligand as in the pentaammine complexes. The cyclic voltammograms (Fig. 4) of the bispyrazine complexes show two discrete reduction steps. It was, however, not confirmed whether the reduction proceeds via a complex which contains a pyrazine and a reduced pyrazine ligand or via a complex which contains two equivalent radical pyrazines. A more detailed study of the reduction products was not attempted. The sharp anodic peak obtained with the trans-complex (Fig. 4) is not observed when the potential sweep is initiated at the peak potential of the first cathodic peak. It might be due to adsorption or deposition of the complex, $HN\langle\rangle NRu(NH_3)_4N\langle\rangle NH$, which is expected as a product of a four-electron reduction of the trans-complex. The new complex has an overall charge of zero. The reason why this complex is adsorbed or deposited on the electrode while the cis-complex appears not to be, might be because of its hydrophobic nature arising from its symmetry and charge.

The reduction potential of free pyrazine in an aqueous solution is strongly dependent on the pH of the solution. The pH dependence of the half-wave potential[26, 30] is different from that observed for the reduction of pyrazine coordinated to ruthenium(II). Therefore, a direct comparison of the reduction potentials of free and coordinated pyrazine in order to see the effect of coordination on the reduction

FIG. 4. Cyclic voltammograms.

1. Cathodic sweep, $Ru(NH_3)_5Pz^{2+}$ in 1 F NaCl
2. Cathodic sweep, cis-$Ru(NH_3)_4Pz_2^{2+}$ in 1 F NaCl
3. Cathodic sweep, trans-$Ru(NH_3)_4Pz_2^{2+}$ in 1 F NaCl
4. Anodic sweep, the same solution as 1
5. Anodic sweep, the same solution as 2
6. Anodic sweep, the same solution as 3

Currents in arbitrary scale

Sweep rate = 10 v/sec

Anodic polarograms were recorded by reversing the potential sweep after recording the cathodic polarograms.

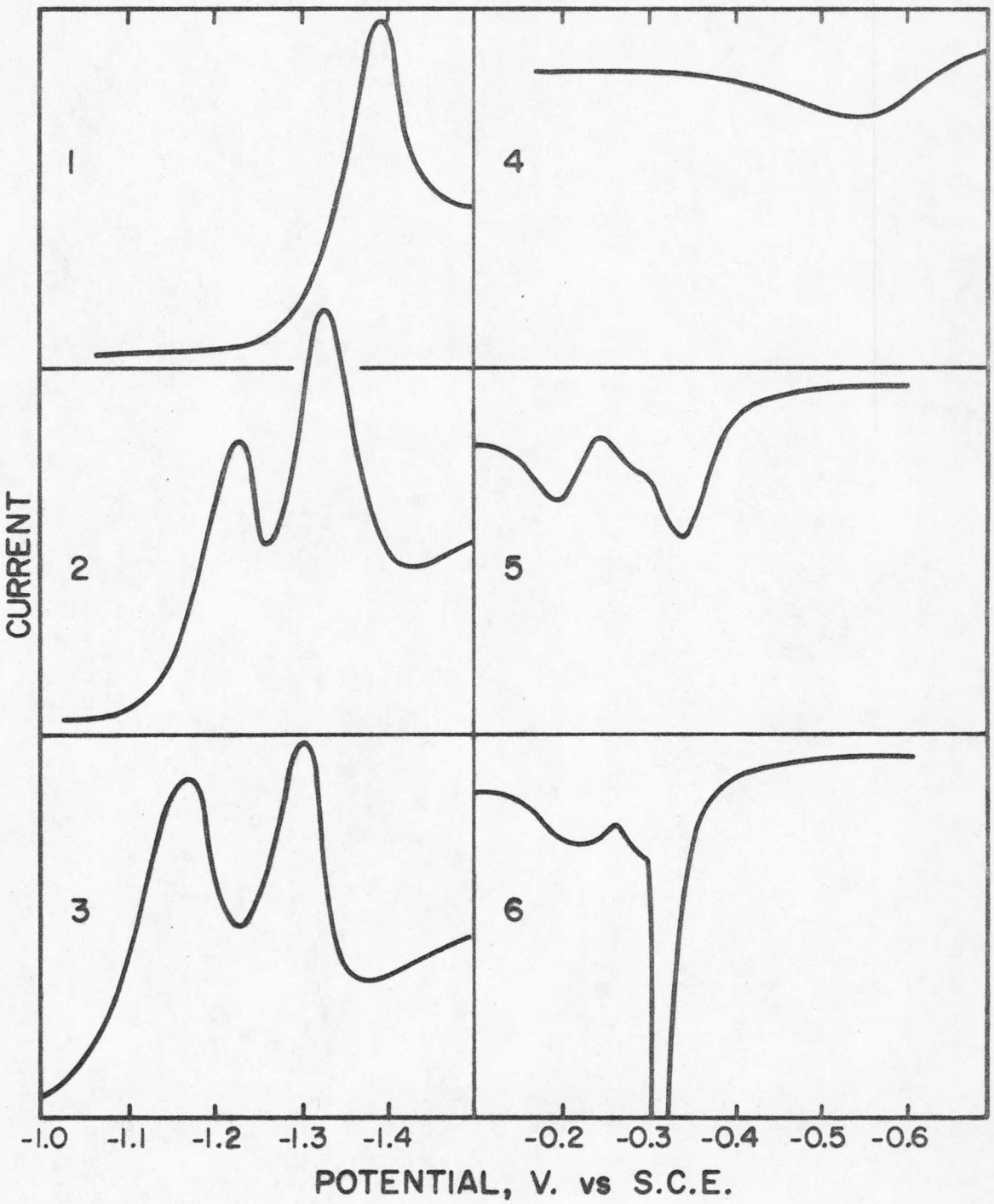
1
2
3
4
5
6
CURRENT
-1.0
-1.1
-1.2
-1.3
-1.4
-0.2
-0.3
-0.4
-0.5
-0.6
POTENTIAL, V. vs S.C.E.

potential is not possible. An attempt has been made to see this effect by measuring reduction potentials of the free and coordinated ($Ru(NH_3)_5Pz^{2+}$) pyrazine in an aprotic media, dimethylsulfoxide (DMSO), but it was thwarted because the polarographic wave of the complex in DMSO was not well defined and, therefore, it was not possible to obtain an unambiguous reduction potential of the coordinated pyrazine.

REFERENCES

1. P. C. Ford, Coordin. Chem. Rev., 5, 75 (1970).
2. J. Masěk, Inorg. Chim. Acta Rev., 3, 99 (1969).
3. L. H. Vogt, Jr., J. L. Katz, and S. E. Wiberley, Inorg. Chem., 4, 1157 (1965).
4. E. L. Farquhar, L. Rusnock, and S. J. Gill, J. Amer. Chem. Soc., 92, 416 (1970).
5. K. Gleu and W. Breuel, Z. anorg. allgem. Chem., 237, 197 (1938); 237, 335 (1938).
6. P. C. Ford, DeF. P. Rudd, R. Gaunder, and H. Taube, J. Amer. Chem. Soc., 90, 1187 (1968).
7. A. M. Zwickel and C. Creutz, private communication.
8. C. Creutz, Ph. D. Thesis, Stanford University, 1970.
9. C. Creutz and H. Taube, J. Amer. Chem. Soc., 91, 3988 (1969).
10. T. Eliades, R. O. Harris, and P. Reinsalu, Can. J. Chem., 47, 3823 (1969).
11. H. S. Lim and F. C. Anson, Inorg. Chem., 10, 103 (1971).
12. H. S. Lim and F. C. Anson, J. Electroanal. Chem., in press.
13. R. S. Nicholson and I. Shain, Anal. Chem., 36, 706 (1964).
14. J. H. Baxendale, R. A. J. Rogers, and M. D. Ward, J. Chem. Soc. (A), 1246 (1970).
15. F. Basolo and R. G. Pearson, "Mechanisms of Inorganic Reactions", 2nd Ed., John Wiley and Sons, Inc., New York, 1967, p. 76.

16. T. W. Kallen and J. E. Earley, Inorg. Chem., 10, 1149 (1971).

17. "Stability Constants of Metal-Ion Complexes" compiled by L. S. Sillen, Special Publication No. 17, London: The Chemical Society, 1964.

18. J. Armor and A. Haim, J. Amer. Chem. Soc., 93, 867 (1971).

19. D. J. Barclay and F. C. Anson, unpublished experiments.

20. F. C. Anson and J. Caja, J. Electrochem. Soc., 117, 306 (1970).

21. D. J. Barclay, E. Passeron, and F. C. Anson, Inorg. Chem., 9, 1024 (1970).

22. A. D. Allen, T. Eliades, R. O. Harris, and P. Reinsalu, Can. J. Chem., 47, 1605 (1969).

23. J. A. Broomhead, F. Basolo, and R. G. Pearson, Inorg. Chem., 3, 826 (1964).

24. J. F. Endicott and H. Taube, Inorg. Chem., 4, 437 (1965).

25. J. N. Armor and H. Taube, J. Amer. Chem. Soc., 91, 6874 (1969).

26. E. D. Moorhead and D. Britton, Anal. Letters, 1, 541 (1968).

27. L. N. Klatt, 15th Annual Report on Research, The Petroleum Research Fund, ACS, 1970, p. 91.

28. A. Albert, "Heterocyclic Chemistry", The Athlone Press, University of London, 1968, Ch. 13.

29. R. A. Sulzbach and A. F. M. Iqbal, Angew. Chem., 83, 145 (1971).

30. J. Volke, D. Dumanović and V. Volková, Coll. Czech. Chem. Commun., 30, 246 (1965).